Ore Geology Reviews 142 (2022) 104697

Contents lists available at ScienceDirect

Ore Geology Reviews

journal homepage: www.elsevier.com/locate/oregeorev

Review

Giant Sb metallogenic belt in South China: A product of Late Mesozoic flat-slab subduction of paleo-Pacific plate

Jun Yan [a,1], Shanling Fu [a,*,1], Shen Liu [b], Luming Wei [a,c], Tianxing Wang [a,c]

[a] State Key Laboratory of Ore Deposit Geochemistry, Institute of Geochemistry, Chinese Academy of Sciences, Guiyang 550081, China
[b] State Key Laboratory of Continental Dynamics and Department of Geology, Northwest University, 229 Taibai Road, Xi'an 710069, China
[c] University of Chinese Academy of Sciences, Beijing 100039, China

ARTICLE INFO

Keywords:
South China Sb Metallogenic Belt
Flat-slab Subduction
West Pacific Plate

ABSTRACT

The giant Sb metallogenic belt in South China (GSMB) has been proved to provide approximately half the world's reserves and Sb production. This metallogenic belt is tectonically located along the transition zone between the Yangtze and Cathaysia blocks, covering an area of ~ 1900 km long and ~ 200 km wide, with a set of large or giant Sb deposits such as the Xikuangshan, Banxi, Woxi, Qinglong, and Banpo-Banian. The Sb deposits have the following features in common: localisation in sedimentary rocks or counterpart metamorphic rocks as veins or strata, structural-tectonic control of mineralisation along the regional NE-trending faults, and the presence of intermediate-mafic dyke rocks in the belt whose relationship with Sb mineralisation is not obvious. Fluid inclusion data show that the Sb mineralisation in this belt generally occurred under low-temperature and low-salinity conditions (140–250 °C, 0.2%–10% $NaCl_{equiv.}$). Abundant isotope data suggest that the Sb deposits in this belt were dominantly generated by crustal fluids from the Proterozoic basement sequences and fresh meteoric water or their mixture with various proportions, whereas the magmatic contribution to Sb mineralisation in this region is a preferential heat source rather than a material supplier (i.e., fluids and metals). The reported geochronological data of representative Sb deposits suggest an age distribution trend of Sb mineralisation, from 120 to 130 Ma in the Xikuangshan, Banxi, Woxi, Banpo and Banian Sb deposits in the northern and central parts of the GSMB, to 140–165 Ma in the Qinglong, Muli and Maxiong Sb deposits in the southern part of this belt. This age trend of the GSMB is largely comparable to that of Mesozoic igneous rocks in the Cathaysia Block, indicating both of them are the products of the west-northwestward flat-slab subduction and post-subduction of the paleo-Pacific Plate during the Late Mesozoic. In combination of the geological, geochemical, and reported geochronological data, we proposed that the Sb deposits in GSMB in South China probably have been mainly generated by low-temperature and low-salinity crustal fluids which leached Sb and S from basement sequences under an extensional setting during Late Mesozoic.

1. Introduction

China ranks the first in the world both for Sb production and reserves (Zaw et al., 2007; Hu et al., 2017a, b; Fu et al., 2020a). The known Sb deposits in China are mainly distributed along transition zones between different tectonic units or regional faults, and constitute a series of Sb metallogenic belts in different regions (Zhang et al., 1998; Wang et al., 2013). Among these belts, >500 Sb deposits with varying scales and grades have been found within the transition zone between the Yangtze and Cathaysia blocks in southern China, which constitute the giant Sb metallogenic belt in South China (i.e., the GSMB; Fig. 1; Xiao et al., 1992; Liu et al., 1998; Wang et al., 2020). However, despite decades of substantial efforts, the timing of Sb mineralisation in this belt remains highly variable because of the absence of suitable minerals for reliable radiometric dating, and a wide range of ages from ~ 420 to ~ 120 Ma has been obtained from various dating methods (Hu et al., 1996; Peng et al., 2008; Wang et al., 2012; Li et al., 2018, 2020; Fu et al., 2019, 2020b; Zhang et al., 2019). Uncertainties over mineralisation ages and the significance of a possible link between tectonic events and abnormal Sb enrichment have hampered the understanding of the genetic model of these deposits in the GSMB.

The South China Block is tectonically bounded by the North China

* Corresponding author.
E-mail address: fushanling@mail.gyig.ac.cn (S. Fu).
[1] Contribute equally.

https://doi.org/10.1016/j.oregeorev.2022.104697
Received 15 August 2021; Received in revised form 3 January 2022; Accepted 4 January 2022
Available online 7 January 2022

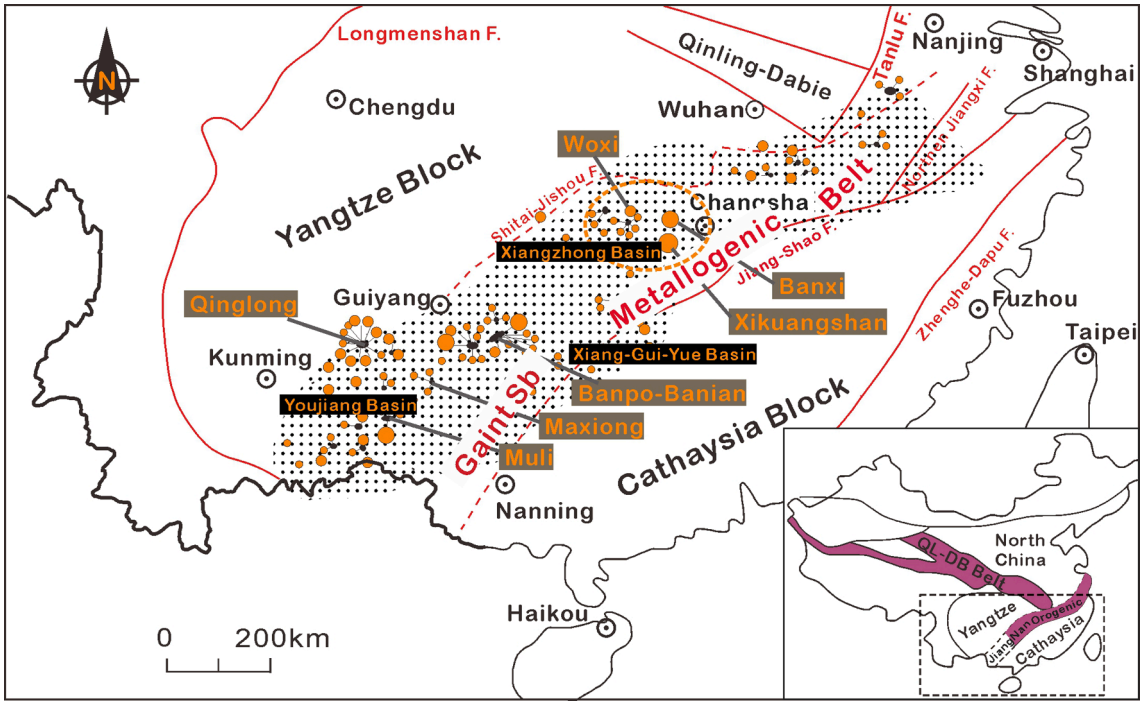

Fig. 1. A simplified geological map of the giant Sb metallogenic belt in South China (GSMB) showing the structural framework and distribution of major Sb deposits in the GSMB (modified from Peng and Hu, 2001; Hu et al., 2017a,b; Wang et al., 2020).

Craton by the Qinling-Dabie orogenic belt and North China Craton to the north, the Tibetan Plateau by the Longmenshan Fault to the northwest, and the Indochina Craton by the Song-Ma Fault to the south (Li and Li, 2007; Wang et al., 2011; Hu and Zhou, 2012; Fig. 1). It comprises the Yangtze and Cathaysia Blocks, which were welded along the Neoproterozoic Jiang-Shao tectonic suture zone, which coincides with the GSMB. The Cathaysia Block is well known for its Mesozoic large-scale granite province with a width of > 1,000 km and granite-related W-Sn polymetallic deposits, which have supplied >50% of the world's W and 20% of Sn reserves (Hu and Zhou, 2012; Sun et al., 2012; Mao et al., 2013). Numerous studies have suggested that the subduction and subsequent post-subduction of the paleo-Pacific plate are responsible for producing large-scale magmatism and W-Sn mineralisation (John et al., 1990; Li and Li, 2007; Zhou and Li, 2000; Zhou et al., 2006; Sun et al., 2007; Wang et al., 2011; Li et al., 2012a,b; Hu and Zhou, 2012; Mao et al., 2013, Mao et al., 2021a, Mao et al., 2021b). However, though a possible link between the Sb mineralisation in the GSMB and large-scale magmatism in the South China Block was also proposed (Peng and Hu, 2001), the detailed relationship between this belt and subduction of the paleo-Pacific plate remains poorly understood.

In the past two decades, abundant new data on Sb deposits in the GSMB have been obtained and demonstrate that Sb deposits in this belt dominantly formed during the Late Mesozoic, although multiple episodes of Sb mineralisation have been identified (Peng and Hu, 2001; Xiao, 2014; Hu et al., 2017a, b; Fu et al., 2016, 2019, 2020a, Fu et al., 2020b; Li et al., 2018, 2020; Zhang et al., 2019). In this study, we compiled and reviewed available data of geological, geochemical and geochronological data of the Sb deposits in the GSMB and presented a comprehensive synthesis of Sb metallogeny in this belt. In compilation with reported geochronological data of Mesozoic granites in South China, we put forward a consistent geodynamic model for the giant Sb metallogenic belt in South China in relation to the flat-slab subduction of paleo-Pacific plate during Late Mesozoic.

2. Geological background

2.1. Regional geology

The Sb metallogenic belt in South China is predominantly located at the southeastern margin of the Yangtze Block and to a lesser extent in the adjacent Cathaysia Block, comprising the traditional Jiangnan orogen and Xiangzhong basin to the north, and the Xiang-Gui-Yue basin and Youjiang basin to the south (Fig. 1; Xiao et al., 1992; Liu et al., 1998; Peng and Hu, 2001; Zhang et al., 2019). This NE-trending metallogenic belt extends approximately 1900 km long and 200 km wide, spanning seven provinces from Anhui to Yunnan (Fig. 1). It has provided more than 83.1% of the total Sb reserves in China, including 9 of 10 large Sb deposits in China and the world's largest Sb deposit at Xikuangshan (Zhang et al., 1998; Hu et al., 2016, 2017a, Hu et al., 2017b; Fu et al., 2020a, Fu et al., 2020b).

The GSMB experienced a complicated geological history as transition zone between the Yangtze and Cathaysia blocks (Liu et al., 1998; Shu, 2006, 2012; Li and Li, 2007; Zhao et al., 2011; Wang et al., 2012; Zhang et al., 2013; Fu, 2015). This history includes the following: (i) The paleo-South China Ocean (Cathaysia) subducted beneath the Yangtze block nucleus (Jinning Terrain) caused the continental collision between the Yangtze and Cathaysia blocks during Early Neoproterozoic (1000 ~ 800 Ma) and resulted in a residual basin in the western part of Jiangshan in the GSMB (850 ~ 800 Ma); (ii) The GSMB underwent continuous intracontinental sedimentation for approximately 400 Ma and the residual basin in South China was broken-up since Late Neoproterozoic, and the Caledonian orogeny during Early Paleozoic resulted in the final convergence of the Yangtze and Cathaysia Blocks in Caledonian; (iii) During Early Mesozoic, the westward subduction of the paleo-Pacific plate underneath the eastern margin of the Eurasian continent caused the formation of voluminous granitic plutons in the Cathaysia Block and eastern part of the Yangtze Block, and the associated deformation might have been caused by the collision between the Indochina and South China block, which is responsible to the closure of Paleotethys; (iv) During the Late Mesozoic Yanshanian event, the subduction and post-subduction of the paleo-Pacific plate beneath the Eurasian continent

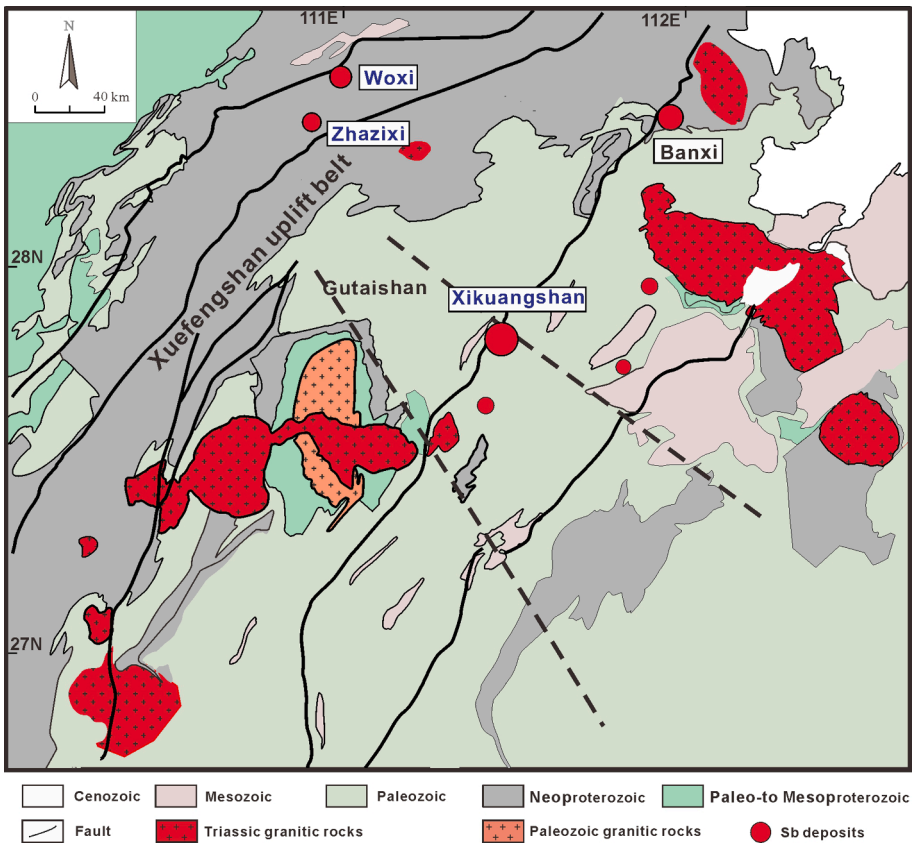

Fig. 2. Geological map of the Xiangzhong basin showing the geological background of the Banxi and Xikuangshan Sb deposits (modified from Hu et al., 2017a,b).

resulted the formation of the giant Yanshanian granitic province with a swath of > 1000 km.

The lithostratigraphic sequences of the GSMB were highly variable. The basement of the Yangtze Block is mainly composed of Neoproterozoic epimetamorphosed rocks (e.g., slates and other metasedimentary rocks) in the east, including the Banxi, Lengjiaxi, Fanjingshan, and Sibao groups. The sedimentary succession consists mainly of Cambrian to Triassic marine sedimentary rocks and Jurassic-Cretaceous and Cenozoic terrigenous sedimentary rocks (Peng and Hu, 2001; Wang et al., 2016; Zhang et al., 2019). In contrast, however, only a small volume of igneous intrusions outcrop in the GSMB. There are sparse granites in the northeastern part of the Jiangnan Orogen belt, with ages from the Neoproterozoic to Early Cretaceous (Wang et al., 2004; Zhong et al., 2005; Peng et al., 2006; Fu, 2015; Li et al., 2015; Wang et al., 2016; Lu et al., 2017). In addition, a few small granitic intrusions and mafic dykes with Mesozoic ages also have been found in the Xiangzhong and Youjiang basins (Hu and Zhou, 2012; Mao et al., 2013; Pi et al., 2017; Zhu et al., 2017). However, the genetic link between these igneous rocks and Sb deposits remains debatable because of no significant spatial association between them.

On a regional scale, the Sb deposits in the northern part of the GSMB are distributed along with the NE- and NNE-trending regional deep faults whereas those in the southern part are distributed with NE- or NW-trending regional faults and mainly controlled by related deposit-scale faults. Host strata of these deposits vary from Neoproterozoic to Tertiary, where host rocks are mainly composed of sedimentary and carbonate rocks and counterpart epimetamorphic rocks.

Considering the reserve and quantity of Sb deposits and tectonic background, three featured regions of Sb mineralisation can be identified, notably, the Xiangzhong basin, Southeast Guizhou Province and the Dian-Qian-Gui area. The Xiangzhong basin is located at the eastern margin of the Yangtze Block (Fig. 1). Sb deposits in this area mostly occur along NE-striking regional structures on the margin and interior of the Xiangzhong basin including the Xikuangshan, Banxi, Woxi, and Zhazixi deposits (Fig. 2). This area underwent continuous sedimentation from the Late Neoproterozoic to Early Paleozoic (Wang and Li, 2003). Ductile shearing, intense folding and granitic magmatism were produced by the Early Paleozoic Caledonian orogeny (Faure et al., 2009; Charvet et al., 2010). Additionally, beaded uplifts such as the Baimashan- Longshan, Weishan-Nanyue and Simingshan-Guandimiao uplifts formed during this period (Liu, 2005; Bai et al., 2013). Subsequently, the Xiangzhong basin formed between these uplifts and sedimentation resumed on the Pre-Devonian metamorphosed clastic strata (Fig. 2), which were unconformably overlain by the Late Paleozoic to Early Mesozoic marine sedimentary sequence (Shi et al., 1993; Ma et al., 2002). In the Late Triassic, the NE-striking regional structures (e.g., the Xuefengshan uplift belt) were produced by the Indosinian orogeny (Shu et al., 2009; Chu et al., 2012a, b; Fig. 2). These regional structures were reactivated and the Xuefengshan belt was further uplifted during the Late Mesozoic tectonic event (Li et al., 2013). The geophysical data suggest that some concealed intrusions might be present at depth although igneous rocks of this period are rarely outcropped in the Xiangzhong basin (Li, 1996; Rao et al., 1999).

The Southeast Guizhou area is a polymetallic mineralisation region containing abundant Sb, Au, and Hg deposits, and is located at the southwestern edge of the Yangtze Block, the area adjacent to the Tethys and Pacific tectonic domain (Xu et al., 2010; Fig. 1). This area is a Paleozoic basin which was covered by a Paleozoic marine carbonatite sequence and underwent multiple tectonic events from Hercynian to Yanshanian (Zheng et al., 2019, Fig. 3A), in which the Dushan Sb ore field, Sandu-Danzhai Hg-Sb-Au ore field, and Leigongshan Sb-Au ore field have been found in this area. Sb deposits in the Dushan Sb ore field, including the Banpo, Banian, Beida and Weizhai deposits mostly occur within secondary faults of the NNE-trending Dushan and Lantu structures (Fig. 3B). Geophysical data suggest that concealed granites might be present at depth in the southeastern part of this area (Diao et al.,

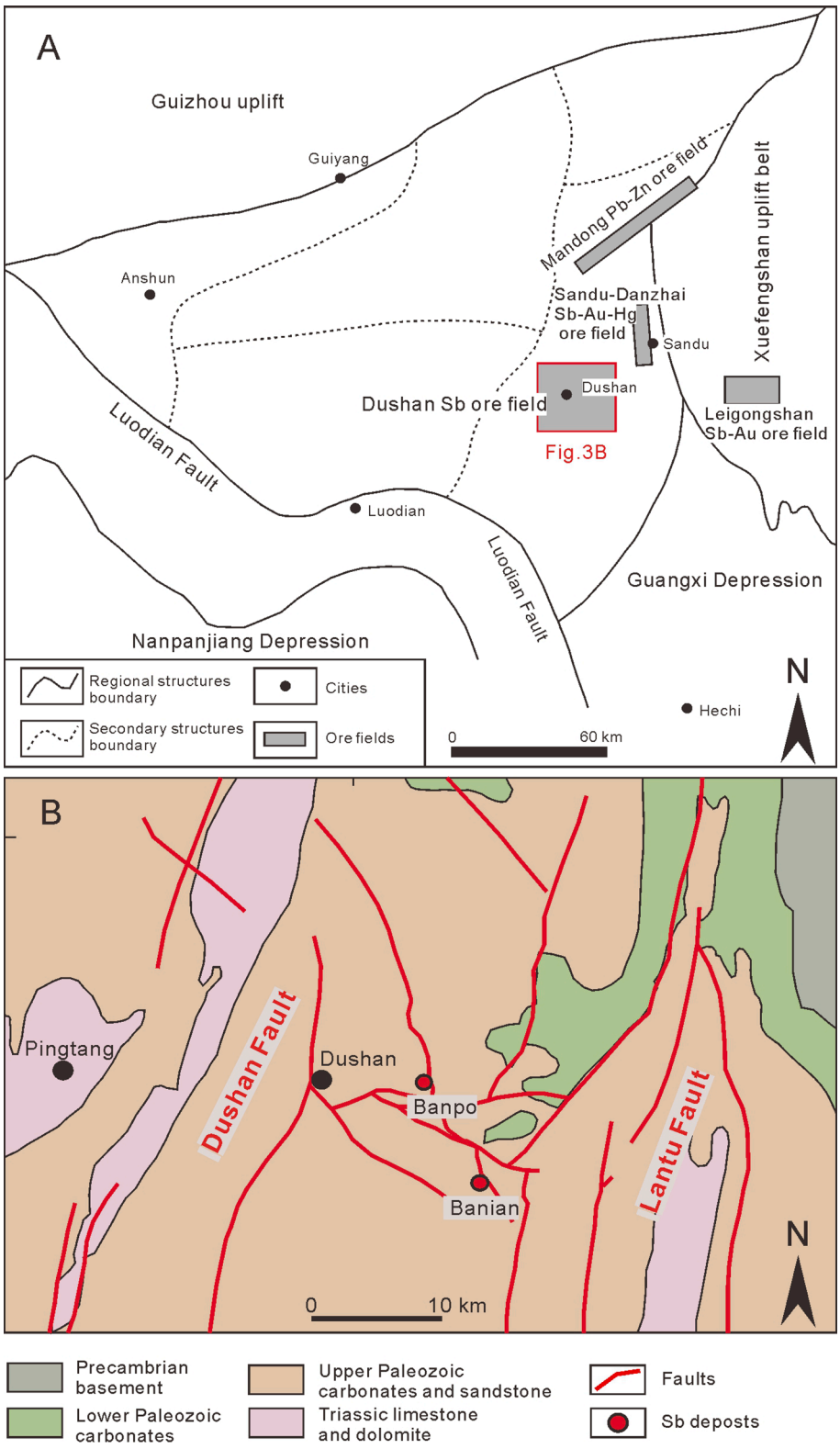

Fig. 3. (A) Geological map of the Southeast Guizhou area showing the geological background of Dushan Sb ore field (after Zheng et al., 2019). (B) Geological map of Dushan Sb ore field and geological background of Banpo and Banian Sb deposits (modified from Zheng et al., 2019).

2017).

The Dian-Qian-Gui area is located at the southwestern margin of the Yangtze Block, and is structurally defined by the Mile-Shizong fault to the northwest, the Shuicheng-Ziyun-Bama fault to the northeast, and the Red River fault to the southwest (Fig. 4; Cai and Zhang, 2009; Yang et al., 2012; Faure et al., 2014). Early studies have suggested that the Dian-Qian-Gui area overlies the basement of Early Paleozoic strata and recorded significant marine sedimentation between the Late Paleozoic and Middle Triassic, experiencing a marine sedimentation with a thickness of *ca.*7000 m (Galfetti et al., 2008; Song et al., 2009; Yang et al., 2012). The marine sedimentary sequence was folded as an EW-trending Youjiang fold and thrust belt by the Indosinian uplift during

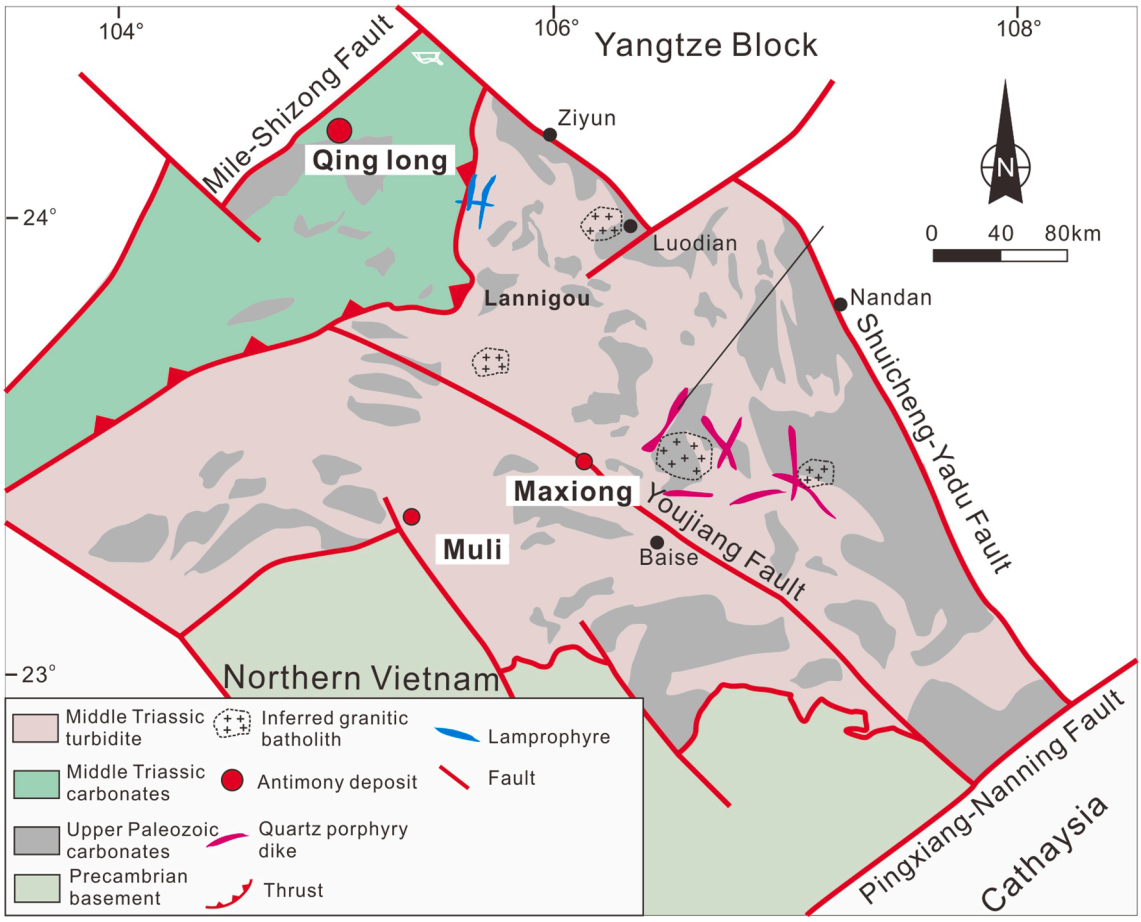

Fig. 4. Geological map of the Dian-Qian-Gui area showing the location and geological background of the Qinglong, Maxiong and Muli Sb deposits (modified from Chen et al., 2018).

the Late Triassic (Cai and Zhang, 2009; Yang et al., 2012). Magmatic rocks occurring in this area mainly include Late Permian dolerites (Zhang and Xiao, 2014), quartz porphyry dykes (Zhu et al., 2016) and lamprophyre dykes (Liu et al., 2010). However, only scarce magmatic rocks are present in known Sb deposits such as the Qinglong, Maxiong and Muli deposits (Wang et al., 2009, Wang et al., 2015).

2.2. Geology of representative Sb deposits

The geological features of most Sb deposits have been described in the literature, and the most important details of representative Sb deposit in the GSMB are summarised as follows. Notably, igneous rocks are rare in each Sb deposit, although some magmatism is observed in the GSMB.

2.2.1. Banxi Sb deposit

The Banxi Sb deposit is situated within the transition zone of the transitional region from the Xuefengshan uplift belt to the Xiangzhong basin (Fig. 2) with a total Sb reserve of ~ 100,000 tons and an average grade of 15.3%–25.9% Sb. This deposit contains two ore blocks, Jiangjiachong and Xiaogang, from south to north. The Neoproterozoic Wuqiangxi Formation of the Banxi Group is the major strata exposed in this deposit, which is lithologically composed of epimetamorphic clastic rocks with original features of littoral facies to neritic facies flysch sedimentary sequences (Fig. 5A). Quartz-porphyry dykes in the northern part of this deposit are the only intrusion rocks with a U-Pb age of ~ 220 Ma, which were cut by quartz-stibnite veins and thus were considered to be earlier than Sb mineralisation (Zhao et al., 2005; Fu et al., 2019). Orebodies of the Banxi deposit mainly occur as veins in the Neoproterozoic epimetamorphic rocks of the Wuqiangxi Formation and are controlled by the NE-trending regional fault F1 (a part of the regional Taojiang-Chengbu fault) and a set of secondary compressional torsional faults with an angle > 70° (Fig. 5A; Li et al., 2018). The ore composition is simple, with stibnite as the principal ore mineral with minor arsenopyrite; the gangue mineral is dominated by quartz. Two types of fluid inclusions were identified in quartz as liquid-rich two-phase inclusions and CO_2-rich inclusions. The fluid inclusion data suggested a low-temperature (170–260 °C) and low-salinity (3%–6% $NaCl_{equiv.}$) metallogenesis (Li et al., 2019). The wall-rock alteration related to Sb mineralisation mainly includes silification, sericitisation and chloritisation (Li et al., 2019).

2.2.2. Xikuangshan Sb deposit

The giant Xikuangshan Sb deposit within the Xiangzhong basin in Hunan Province is situated at the intersection of the NE-trending Taojiang-Chengbu and NW-trending Xikuangshan-Lianyuan basement faults (Fig. 2) with a total Sb metal reserve of ~ 2.5 Mt and an average grade of ~ 4% Sb. The dominated host rocks in the Xikuangshan deposit are Middle to Upper Devonian and Lower Carboniferous strata, which are mainly composed of carbonates and locally interbedded with siltstone, argillite, and shale (Fan et al., 2004; Peng et al., 2003a). These strata have been intensely deformed into a kilometre-scale, NNE-trending major fold structure referred to as the Xikuangshan complex anticline (Fig. 5B; Peng et al., 2003a; Yang et al., 2006). Fault F_{75} (a part of the Taojiang-Chengbu regional fault) cuts the northwest limb of the anticline, and almost all ore-bodies occur in the footwall of this fault (Fig. 5B). A NNE-trending lamprophyre dyke with a length of ~ 10 km is the only outcropping intrusive rock in the Xikuangshan deposit (Fan

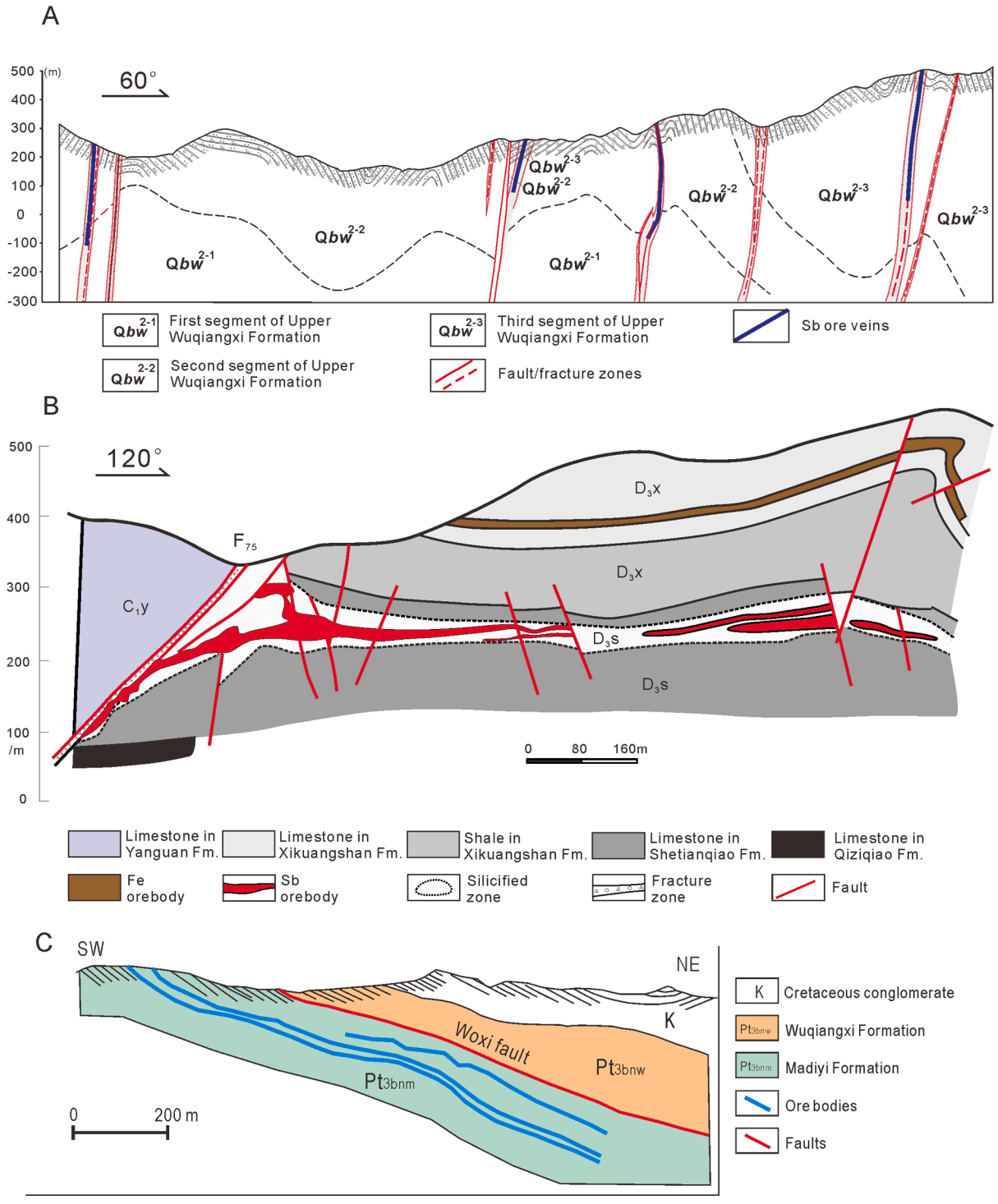

Fig. 5. (A) Cross-section map of Banxi Sb deposit showing the ore body veins controlled by high-angle faults (after Li et al., 2018). (B) Cross section map of the Xikuangshan Sb deposit (modified from Yang et al., 2006). (C) Cross section map of Woxi Sb deposit (modified from Gu et al., 2012).

et al., 2004; Hu et al., 1996; Peng et al., 2003a). The Sb mineralisation in the Xikuangshan deposit consists of four ore blocks, referred to as Laokuangshan, Tongjiayuan, Wuhua, and Feishuiyan (Hu et al., 1996; Peng et al., 2003a). Orebodies mainly occur as stratiform and are strictly controlled by interlayer fault zones in silicified carbonates (Fig. 5B). Ore minerals in this deposit are primarily composed of stibnite with trace disseminated pyrite, and gangue minerals are dominated by quartz and calcite with minor barite, fluorite, and talc (Fan et al., 2004; Fu et al., 2020a; Hu et al., 1996; Hu and Peng, 2018; Peng et al., 2003a). Four types of fluid inclusions in the Xikuangshan Sb deposit were identified in quartz, fluorite, barite and stibnite including pure liquid phase, liquid-rich aqueous phase, vapour-rich aqueous phase and pure vapour phase. The fluid inclusion data suggested a low to meso-thermal (112–366 °C) and low salinity (0.2%–15.4% $NaCl_{equiv.}$) ore-forming fluid. (Hu and Peng, 2018). Silicic alteration is the primary wall- rock alteration in the deposit and Sb orebodies never appear to exceed the limit of silicification zone (Hu et al., 1996; Yang et al., 2006). A lamprophyre dyke occurs in the eastern part of the orebodies as the eastern

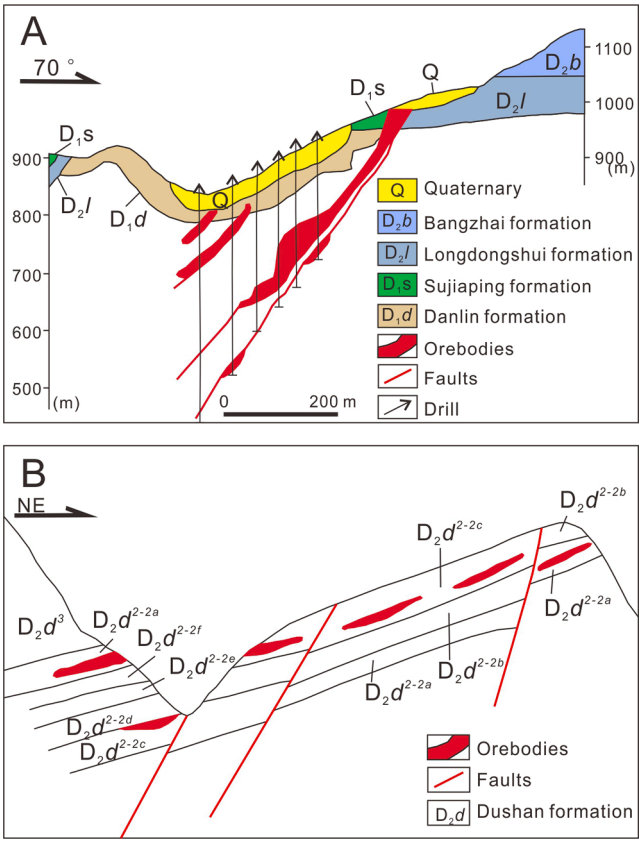

Fig. 6. (A) Cross-section map of Banpo Sb deposit showing that orebodies occur in Danlin formation (D_1d) sandstone and argillaceous siltstone and are controlled by faults (after Zheng et al., 2019). (B) Cross-section map of Banian Sb deposit showing that orebodies occur in the interface of carbonatite and clasolite in Dushan formation (D_2d) (after Xue et al., 2019).

boundary of antimony mineralisation in the Xikuangshan ore district (Liu and Jian, 1983; Shi et al., 1993).

2.2.3. Woxi Sb polymetallic deposit

The Woxi Sb polymetallic deposit is situated in the northeast corner of Xuefengshan uplift belt in western Hunan province, China, which contains five ore blocks including Hongyanxi, Yuershan, Lijiaxi, Shiliupenggong, and Upper Woxi (Fig. 2; Gu et al., 2012; Zhu and Peng, 2015). The metal reserves for the Woxi deposit amount to 0.22 Mt of Sb, >50 t of Au, and 25,000 t of WO_3, and the average grades of Sb, Au, W in the ores are 2.84%, 9.77 ppm and 0.3%, respectively. The dominated strata exposed in the Woxi region consist of the Proterozoic Lengjiaxi Group, Banxi Group and Cretaceous conglomerate. The Banxi Group is composed of Madiyi Formation and Wuqiangxi Formation. The Madiyi formation consist of low-grade metamorphic purple-red sericite slate, sandstone slate and calcareous sericitic slate. The orebodies in this deposit occur in the purple-red calcareous sericitic slate as quartz veins and are controlled by interlay Woxi faults (Fig. 5C; Gu et al., 2012). These quartz veins can be divided into banded vein, veinlet and discordant vein, and the banded vein provides about 70% of metal accumulation (Luo et al., 1984). Ore minerals are dominated by scheelite, pyrite, stibnite, native gold and wolframite with minor arsenopyrite, sphalerite and galena. The gangue minerals consist of quartz with minor sericite, carbonate and chlorite. The mineral paragenesis for this deposit was divided into four stages, including quartz-carbonate stage, quartz-scheelite stage, quartz-sulfide-gold stage, and late quartz-carbonate stage (Zhu and Peng, 2015). Fluid inclusion data yield homogenization temperatures of 180–240 °C at quartz-scheelite veins with 2.41%–5.56% $NaCl_{equiv}$ salinity, and 140–200 °C at quartz-sulfide-gold stage with a 0.88%–6.88% $NaCl_{equiv}$ salinity. It suggested a low-salinity, low-to-moderate temperature ore fluid, consistent with other gold deposits in the Xuefengshan uplift belt (Zhu and Peng, 2015). The magmatic activities are absent in the mining area or adjacent regions.

2.2.4. Banpo-Banian Sb ore field

The Banpo-Banian Sb ore field is situated in southeast Guizhou, which contains two large Sb deposits of Banpo and Banian and a set of other medium-small scale Sb deposits, with a total Sb reverse of >200,000 tons (Diao et al., 2017). The dominant wall-rocks comprise Paleozoic carbonates and sandstone and Triassic limestone and dolomite, which are overlain on the Precambrian epimetamorphic rocks. The structural frame of this area is defined by the NE-trending Lantu Fault and Dushan Fault which is southern part of Songtao-Dushan regional fault. The Banpo and Banian Sb deposits were strictly controlled by the NNW-trending Dushan Fault (Fig. 3B). Sb mineralisation is mainly hosted in Devonian marine sedimentary rocks in the form of quartz-stibnite veins (Fig. 6; Xiao, 2014; Xue et al., 2019). The ore minerals are dominated by stibnite with trace pyrite, cinnabar, realgar and gangue minerals mainly quartz, calcite, dolomite, clay and barite (Shen et al., 2013; Xiao, 2014). Fluid inclusions occurring in quartz and calcite suggest a low temperature (120–180 °C) and low salinity (1.8%–8.3% $NaCl_{equiv.}$) ore-forming fluid. (Wang, 1995) Carbonization and silicification are the primary wall-rock alterations related to Sb mineralisation in these deposits.

2.2.5. Qinglong Sb deposit

The Qinglong Sb deposit is in the northwestern part of the Dian-Qian-Gui area and contains eight ore blocks, including Dachang, Shuijingwan, Dishuiyan, Gulu, Houpo, Xishe, Sanwangping and Heishanjing. The proved total Sb reserve of this deposit is up to 0.27 Mt with an average grade of 2.6% Sb. Local strata outcropping in the deposit area are composed of carbonate rocks of the Maokou Formation and "Dachang" layer of Middle Permian, E'meishan basalt of Upper Permian, and sandstone and shale of the Longtan Formation (Fig. 7A), of which Sb mineralisation is mainly hosted in the "Dachang layer" as quartz-stibnite veins. The "Dachang layer" is lithologically composed of tuff, silicified breccia, which overlays the limestone of the Maokou Formation and is covered by E'meishan basalt. The ore-controlling regional fault in the deposit is the NE-trending Mile-Shizong fault (Fig. 4), which controlled the distribution and occurrence of ore blocks (Fig. 7A; Peng et al., 2003b; Chen et al., 2018). The Qinglong deposit contains several ore blocks, including Gulu, Zhimi, Houpo, Heishanjing, Xishe and Dachang. Individual orebodies range from 50 to 610 m long and 40 to 120 m wide, dipping at 3°–8° to the northwest. The primary ore minerals are composed of euhedral-subhedral stibnite, arsenian pyrite and fine-grained stibnite, and the gangue minerals are mainly jasperoid quartz, fluorite and barite. Ore-forming fluid is characterised by low temperature (130–195 °C) and low salinity (4.3%–8.1% $NaCl_{equiv.}$) (Cai et al., 1997). Wall-rock alterations associated with Sb mineralisation include silicification and kaolinisation.

2.2.6. Maxiong Sb deposit

The Maxiong Sb deposit is in the southeastern part of the Dian-Qian-Gui area, which includes three ore blocks of the Maxiong, Poyan and Kagu with a total Sb reserve of ~ 56,400 tons and an average grade of ~ 5.4% Sb. Tectonically, the deposit is situated at the western margin of the Youjiang rift valley in the transitional area between the Yangtze and Cathaysia blocks. The orebodies are mainly hosted in the unconformity between the Cambrian dolomite and the Upper Devonian Yujiang Formation muddy-carbonaceous clasolite and are controlled by NW-trending compression and scissor faults in the southwest wing of Maxiong anticline (Fig. 7B). The orebodies occur as irregular veins and lenses with a total length of 3200 m and dipping at 50°–80° to the northwest. The primary ore minerals are composed of stibnite with trace pyrite and arsenopyrite and the gangue minerals are mainly quartz and

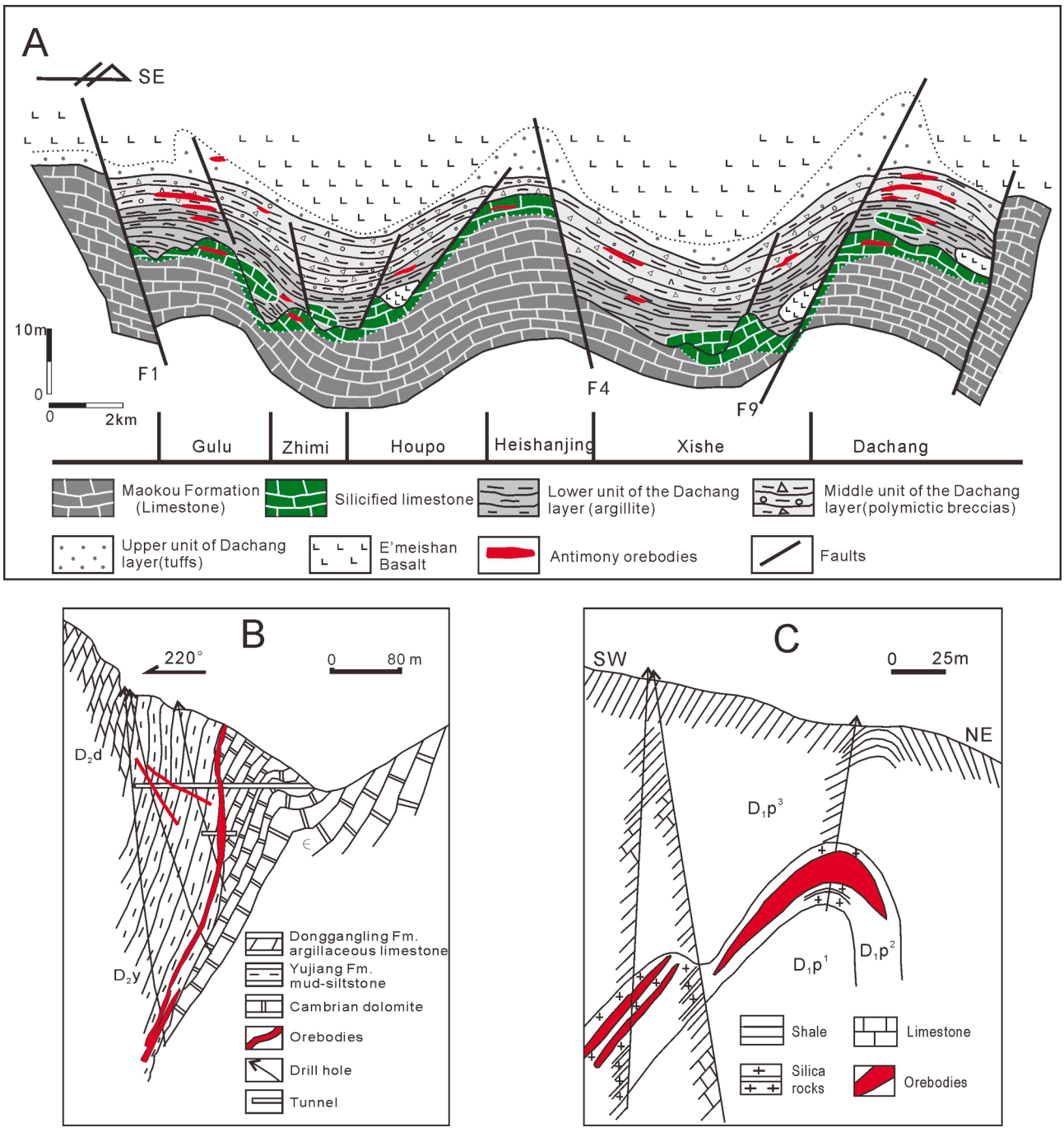

Fig. 7. (A) Cross-section map of Qinglong Sb deposit showing that orebodies mainly occur in the Dachang layer near major faults (after Chen et al., 2018). (B) Cross section of Maxiong Sb deposit showing that orebodies occur in the unconformity between the Cambrian and the Upper Devonian (after Wei, 1993). (C) Cross section of Muli Sb deposit showing that orebodies occur in silica rocks (after Wang and Jin, 1994).

minor calcite. Stibnite mainly occurs as grains with quartz, and minor columnar and acicular stibnite occurs in vein quartz (Wei, 1993). Ore-forming fluids revealed by fluid inclusions from quartz are characterised by low temperature (141–210 °C) and low salinity (6.6%-10.1% $NaCl_{equiv.}$; Cai et al., 1997). Wall-rock alterations are dominated by extensive silicification.

2.2.7. *Muli Sb deposit*

The Muli Sb deposit is in the southwestern part of the Dian-Qian-Gui area and the central part of the Dian-Qian intercontinental rift valley, which is part of the ancient Yangtze Block margin rift (Wang, 1994). The stratigraphy in this area is semi-deep to shallow water shelf faces ranging from the Lower Devonian to Middle Triassic carbonate and shale. The orebodies are mainly hosted in Devonian Pojiao (D_1p) thick-bedded silica rocks with multiple folds controlled by NW-trending faults (Fig. 7C). The total Sb reserve is approximately 0.17 Mt with an average grade of 5.2% Sb. The orebodies occur as veins and lenses and are consistent with the stratum attitude. The primary ore mineral is stibnite associated with pyrite, quartz, calcite and barite. Calcite mainly occurs in metallogenic fault structures in the late or post-ore stage (Han et al., 2019). Fluid inclusions from quartz and calcite suggest a low temperature (95–196 °C) and low salinity ore-forming fluid (3.7%–8.8% $NaCl_{equiv}$) (Cai et al., 1997). Silification is the majority wall-rock alteration which is close to the Sb mineralisation (Fig. 7C).

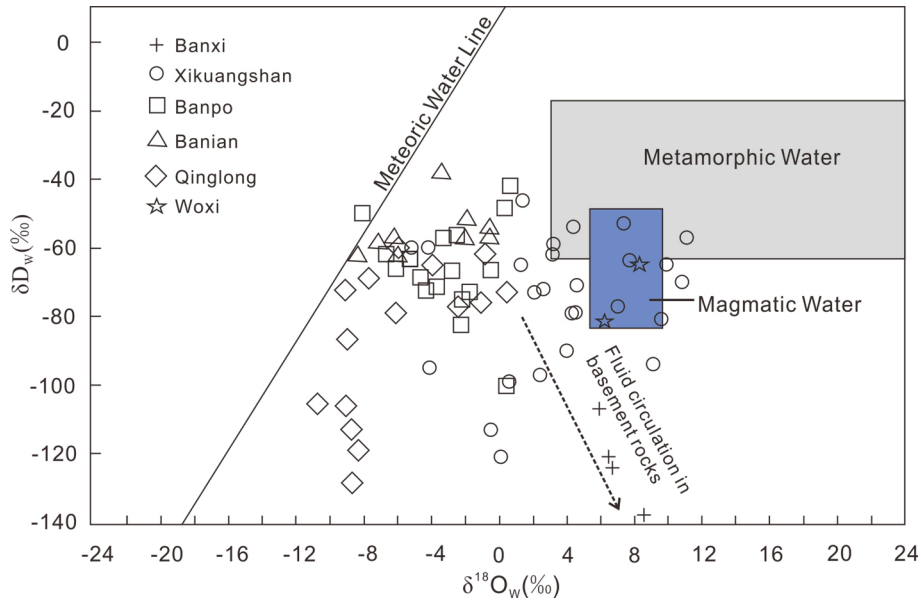

Fig. 8. The δD-$\delta^{18}O$ diagram for ore-forming fluids from Sb deposits in the GSMB. Data sources: Banxi: Li et al. (2019); Xikuangshan: Xie et al. (1996), Yang et al. (1998), Yin and Dai (1999), Peng et al. (2002), Ma et al. (2003), Lin (2014);Woxi: Yang (1986), Liang and Zhang (1986); Banpo: Pan and Wu (2017); Banian: Pan and Wu (2017); Qinglong: Pan and Wu (2017).

3. Timing of Sb mineralisation in the GSMB

Precisely determining the timing of mineralisation is critical for constraining the ore genesis of hydrothermal deposits. However, the precise ages of Sb deposits in the GSMB remain scarce because of the absence of suitable minerals for traditional radiometric dating (Hu et al., 2017b; Fu et al., 2020b). Many Sb deposits in this belt have been mined for more than a century (e.g., Xikuangshan and Banxi) and widely studied by geologists for decades, but few studies have investigated the precise ages of Sb deposits because of the simple mineral assemblages. Over the past two decades, a wide range of Sb mineralisation ages from *ca.* 420 Ma to *ca.* 50 Ma have been determined by applying various radio-isotope dating methods such as Pb-Pb, K-Ar, $^{40}Ar/^{39}Ar$, Rb-Sr, Re-Os, Sm-Nd, (U-Th)/He and electron spin resonance. On the basis of the methods and samples used, the reported ages of Sb mineralisation using different methods must be evaluated with caution. For example, Pb-Pb dating of sulfide minerals is widely recognised as unreliable, particularly in low-Pb systems such as those of Sb deposits in the GSMB, thus, they are not considered in this study.

In this study, we mainly reviewed and investigated the mineralisation ages of these representative Sb deposits obtained by Sm-Nd, Ar-Ar, Rb-Sr and (U-Th)/He radio-isotope dating methods. For example, multiple dating methods, including hydrothermal calcite and stibnite Sm-Nd isochron and zircon (U-Th)/He dating, have been employed to determine the mineralisation age of the giant Xikuangshan Sb deposit in the Xiangzhong basin and yielded an age range of 120–155 Ma (Hu et al., 1996; Fu et al., 2020b). An age of *ca.*130 Ma of the Banxi Sb deposit was obtained using Rr-Sr isochrons of major ore minerals such as stibnite, arsenopyrite, and zircon (U-Th)/He dates (Li et al., 2018; Fu et al., 2019). More recently, an age of *ca.* 130 Ma of the Woxi deposit was also obtained using scheelite and wolframite U-Pb dates (unpublished data). In the southeast Guizhou area, Sm-Nd isochrons of hydrothermal calcite were used to date the Banpo and Banian Sb deposits in the Dushan ore field and yielded ages of 130 Ma and 126–128 Ma, respectively (Wang, 2012; Xiao, 2014). In comparison, however, the mineralisation ages of Sb deposits in the Dian-Qian-Gui area were slightly older. For example, Peng et al. (2003b) proposed the Qinglong Sb deposit formed at 142–148 Ma using Sm-Nd dating of hydrothermal fluorite from ore veins. The Maxiong Sb deposit was dated at 141–156 Ma using K-Ar and Rb-Sr isochron methods of quartz from quartz-stibnite veins (Wei, 1993) while the Muli Sb deposit was dated at *ca.*165 Ma using Ar-Ar isochrons of hydrothermal quartz (Hu et al., 2007; Han et al., 2019).

In summary, the aforementioned age data of representative Sb deposits indicate that Sb mineralization in the GSMB mainly took place during the Late Mesozoic (160 –120 Ma), and a possible age distribution trend of Sb mineralisation in GSMB was also identified, i.e., from *ca.* 120–130 Ma for Sb deposits in the central and northeastern part of this belt (e.g., Xikuangshan, Banxi, Woxi, Banpo, and Banian deposits) to *ca.* 140–165 Ma for Sb deposits in the southwestern part (e.g., the Qinglong, Muli and Maxiong deposits; Fig. 11B). Notably, however, more geochronological studies using robust dating methods are required to further constrain the precise timing of large-scale Sb mineralisation in the GSMB.

4. Origin of Sb deposits in the GSMB

The origin of the Sb deposits in South China has long been debated and various viewpoints have been invoked including intrusion-related and intrusion-unrelated models (Hu et al., 2017a; Chen et al., 2018; Zhang et al., 2020; and references therein). Continuing argument in this respect is driven principally by uncertainties over the significance of a possible magmatic link with Sb mineralisation. Over the past two decades, abundant new data including fluid inclusion, stable isotopes, noble gas, and other geochemical data, have been obtained that enable improvement in understanding the origin of these Sb deposits.

Fluid inclusion studies suggest that ore-forming fluids of Sb deposits in the GSMB are generally characterised by low temperature (average temperature with 140–250 °C) and low salinity (0.2%-10% $NaCl_{equiv.}$) (Wang and Jin, 1994; Wang and Cui, 1996; Cai et al., 1997; Shen et al., 2008; Su et al., 2015; Hu and Peng, 2018; Chen et al., 2018; Li et al., 2019). The fluid inclusion data of each Sb deposit revealed an increasing trend of mineralisation temperature of Sb deposits in the GSMB from southwest to northeast, 95–210 °C for those in the Dian-Qian-Gui area, 120–180 °C for those in Southeast Guizhou area, and 112–366 °C for those in the Xiangzhong basin. In general, the δD_{VSMOW}-$\delta^{18}O$ composition can place a first-order constraint on the origin of the ore-forming fluids for hydrothermal deposits. The δD_{VSMOW} and $\delta^{18}O$ values of ore-forming fluids for Sb deposits in the GSMB calculated from fluid

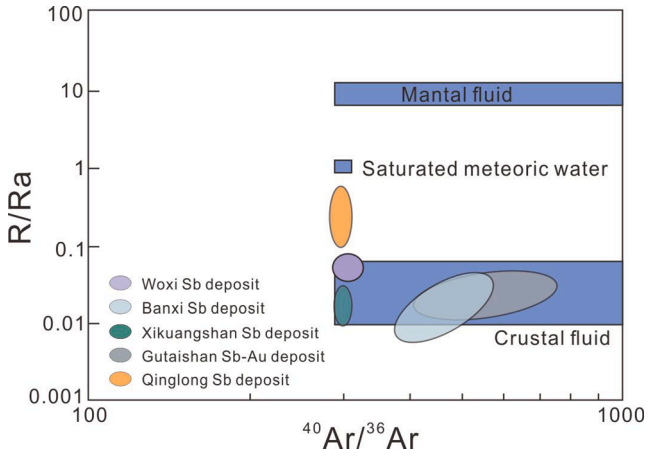

Fig. 9. Plot of $^{40}Ar/^{36}Ar$ vs. R/Ra for representative Sb deposits in the GSMB. Data source: Woxi: Hu, 2021; Banxi: Li et al., 2018; Xikuangshan: Hu, 2021; Gutaishan: Sun et al., 2020; Qinglong: Chen et al., 2016.

inclusions in ore-related hydrothermal minerals range from −128‰ to −46‰ and −10.2‰ to + 11.9‰, respectively (Wang, 1995; Xie et al., 1996; Yang et al., 1998; Yin and Dai, 1999; Peng et al., 2002; Ma et al., 2003; Gu et al., 2012; Lin, 2014; Zhu and Peng, 2015; Hu et al., 2016; Pan and Wu, 2017; Li et al., 2019). In a δD_{VSMOW}-$\delta^{18}O$ diagram of fluid inclusions trapped in hydrothermal quartz and calcite, most samples from representative Sb deposits plot within the transition field of meteoric water and magmatic/metamorphic water (Fig. 8), indicating a mixing origin of ore-forming fluids, i.e., admixture of magmatic or metamorphic water and meteoric water. However, because the latest metamorphic event documented in this district (460–400 Ma; Faure et al., 2009; Wang et al., 2010) occurred many hundred millions of years ago before the timing of Sb mineralisation in the GSMB, metamorphic fluids thus are unlikely to be candidates as one end-member of ore-forming fluids. In addition, the majority of large Sb deposits is primarily hosted in Neoproterozoic epimetamorphic clastic rocks or Devonian-Carboniferous sedimentary rocks, with no obvious direct spatial relationship to magmatic activity, indicating that magmatic fluids seem unlikely to be the major component of ore-forming fluids for these Sb deposits. Recent experiment study demonstrated that weak partitioning of Sb into magmatic fluids makes it unlikely that primary magmatic fluids serve as the Sb source of large epithermal Sb deposits (Fu et al., 2020c). Alternatively, the Mesozoic meteoric water can be one of the end members of ore-forming fluid sources since lots of H-O isotope plots of all investigated Sb deposits are close to the meteoric water line (Hu et al, 2016; Pan and Wu, 2017). The other end member could be interpreted as a result of water–rock interaction between meteoric water and $\delta^{18}O$-enriched wall rocks or $\delta^{18}O$-enriched basement rock (Peng et al., 2014; Hu et al., 2017a), which can be further favoured by following He-Ar isotopic data.

Argon and He isotope ratios in fluid inclusions entrapped hydrothermal sulfide minerals such as pyrite and stibnite have been proved effective for identifying the sources of ore-forming fluids for hydrothermal deposits because of the significant difference in $^{3}He/^{4}He$ and $^{40}Ar/^{36}Ar$ ratios for fluids derived from different geochemical reservoirs (Stuart et al., 1994; Burnard et al., 1999; Burnard and Polya, 2004; Davidheiser-Kroll et al., 2014). For example, crustal fluids are characterised by low $^{3}He/^{4}He$ (0.01–0.05 Ra, where Ra is the atmospheric $^{3}He/^{4}He$ ratio, 1.39×10^{-6}) while the $^{3}He/^{4}He$ of mantle-derived fluids can be up to 6–9 Ra (Burnard et al., 1999; Hu et al., 2009; Mark et al., 2011). The $^{3}He/^{4}He$ values for ore-forming fluids from the Banxi and Qinglong Sb deposits are ranging from 0.01 to 0.03 Ra and 0.13–0.46 Ra, respectively (Chen et al., 2016; Li et al., 2018), which are close to that of crustal fluids but much lower than mantle-derived fluids. This indicates that the ore-forming fluids of these Sb deposits were

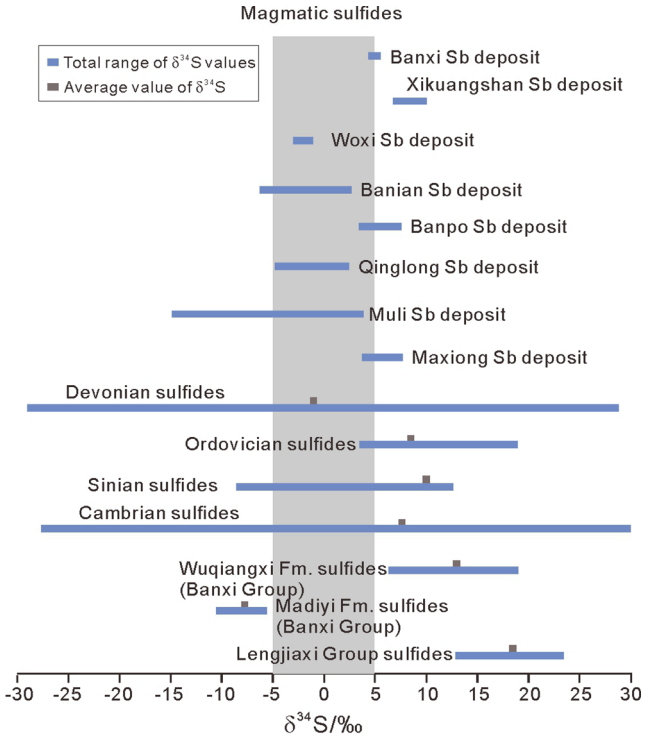

Fig. 10. Sulfur isotopic composition of representative Sb deposits in the GSMB. Data sources: Banxi: Li et al. (2018); Xikuangshan: Fu et al. (2020a); Woxi: Gu et al. (2004, Gu et al., 2012); Banian and Banpo: Cui (1992, 1995), Wang (1995), Shen et al. (2013); Qinglong: Chen et al. (2018), Shen et al. (2013); Maxiong: Shen et al. (2013).

dominantly generated from crustal fluids. Accordingly, the $^{40}Ar/^{36}Ar$ values are range from 409 to 545 and 305–326, respectively (Chen et al., 2016; Li et al., 2018), which are comparable to those of air-saturated water (meteoric), implying that ore-forming fluids are probably dominated by Mesozoic meteoric water. In the $^{3}He/^{4}He$-$^{40}Ar/^{36}Ar$ diagram (Fig. 9), all samples from the Banxi deposit plot within the field of crustal fluid, whereas most samples from the Qinglong deposit plot in the field between crustal fluids and air-saturated water. More recently, Hu (2021) proposed that ore-forming fluids of the giant Xikuangshan Sb deposit are also dominated by Mesozoic modified air-saturated meteoric water based on similar He-Ar isotopic compositions. Therefore, the ore-forming fluids of the Sb deposits in the GSMB were likely to be dominated by Mesozoic meteoric water but were compositionally modified by fluid-rock interaction during the evolution of fluids.

The sulfur isotopic composition of a sulfide deposit can be variable because of multiple possible sources of sulfur in the metallogenetic environment, thus, sulfur isotopes can provide insights into the origins of sulfide minerals in hydrothermal deposits (Ohmoto and Rye, 1979; Hoefs, 2009). Advances in analytical methods, particularly in micro-analytical techniques (e.g., LA-ICP-MS), enable new sulfur isotope data of some representative Sb deposits in the GSMB to be obtained. The S isotope compositions of Sb deposits in the GSMB are shown in the Fig. 10, ranging from 4.8‰ to 6.7‰ in Banxi, 6.8‰ to 10.2‰ in Xikuangshan, −2.8‰ to −1.2‰ in Woxi deposit, −6.3‰ to 2.6‰ in Banian, 3.4‰ to 7.5‰ in Banpo, −5.0‰ to 2.3‰ in Qinglong, −14.5‰ to 3.8‰ in Muli and 3.6‰ to 7.7‰ in Maxiong (Cui, 1992, 1995; Wang, 1995; Gu et al., 2004, 2012; Shen et al., 2013; Hu et al., 2016; Li et al., 2018; Chen et al., 2018; Fu et al., 2020a). The wide range of $\delta^{34}S$ values of the fluid in these deposits indicates a complex source of sulfur in different Sb deposits. The $\delta^{34}S_{V\text{-}CDT}$ values of deposits in the Xiangzhong basin, such as Banxi, Xikuangshan and Woxi show a narrow range, whereas the $\delta^{34}S_{V\text{-}CDT}$ values of deposits such as Banian-Banpo, Qinglong and Muli in southeast Guizhou and the Dian-Qian-Gui area range

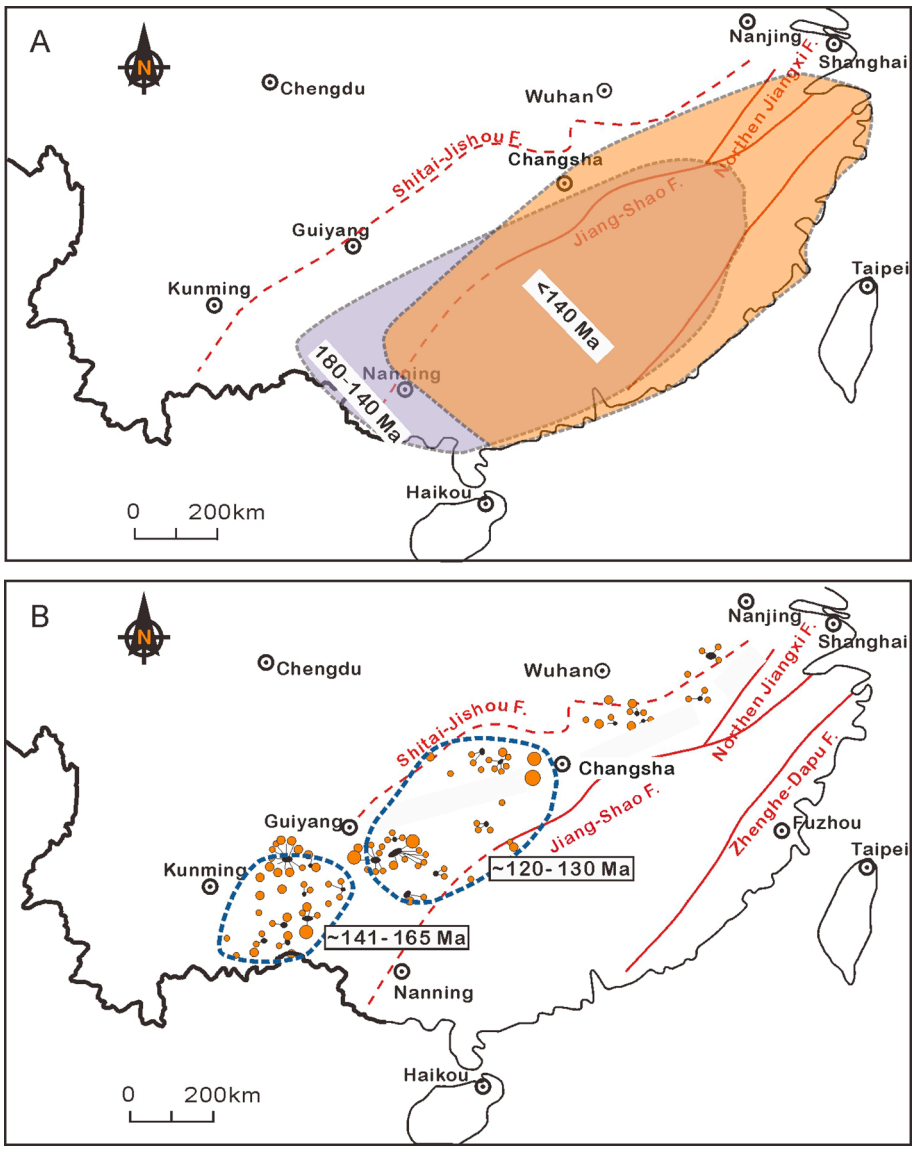

Fig. 11. (A) Distribution of Mesozoic igneous rocks in South China with progressively younger age northeastwards (after Wang et al., 2011; Zhou et al., 2006; Zhu et al., 2016, Zhu et al., 2017). (B) Chronology of the Xiangzhong basin, the Southeast Guizhou area, and the Dian-Qian-Gui area showing a similar younger trend as the chronology of Mesozoic igneous in South China.

within a wider range (Fig. 10). The wide $\delta^{34}S_{V\text{-}CDT}$ values of Sb deposits in the GSMB can be generated by mixing between wall-rocks and magmatic sulfur, or dissolution of sulfides in basement sequences (Hu et al., 2017a; Li et al., 2018, 2019; Fu et al., 2020a). However, as discussed above, the H-O isotope and He-Ar isotopes and the absence of magmatic rocks in ore field suggest that the input of magmatic sulfur into the Sb deposits is insignificant. Trace elements and isotope geochemical data of Precambrian sedimentary strata in South China (Ma et al., 2002, 2003; Ma, 2008; Xu et al., 2012) revealed that the Proterozoic strata are generally enriched of W, Sn, Sb, and Au. The ore-forming metals in Proterozoic basement strata might have been pre-concentrated during previous magmatic events during early tectonic events (Hu, 2021). Therefore, it can be inferred that Proterozoic basement strata could have been the potential sulfur source of these deposits in the Sb belt (Ma, 2008; Hu et al., 2016; Fu et al., 2020a; Hu, 2021 and references therein).

In conclusion, Sb deposits in the GSMB may have formed from evolved meteoric water, which circulated through regional faults and leached Sb and S from the basement metamorphic rocks because of the interaction between the rocks and circulating meteoric fluids. By contrast, deep-seated magmas may have served as heat sources for the circulation and transportation of Mesozoic meteoric water along regional faults (Hu et al., 2017a).

5. Possible link between the paleo-Pacific plate subduction and Sb mineralisation

Extensive magmatism in South China produced one of the largest magmatic provinces worldwide by widespread igneous rocks consisting of granites, rhyolites and subordinate mafic intrusions and volcanic rocks (Li and Li, 2007; Hu and Zhou, 2012; Mao et al., 2013, Mao et al., 2021a, Mao et al., 2021b; Wang et al., 2016). Geochronological data indicate that the magmatic events in South China mainly occurred during the Indosinian Period (251–205 Ma), Early Yanshanian Period (180–150 Ma), and Late Yanshanian Period (140–70 Ma) (Zhou et al., 2006; Wong et al., 2009; Wang et al., 2011; Li et al., 2011). The spatiotemporal distribution of Mesozoic igneous rocks reveals an increasing density and a younger trend toward the ocean (southeastward) (Li and Li, 2007; Li et al., 2007). Additionally, the distribution of igneous rocks with progressively younger northeastwards was also

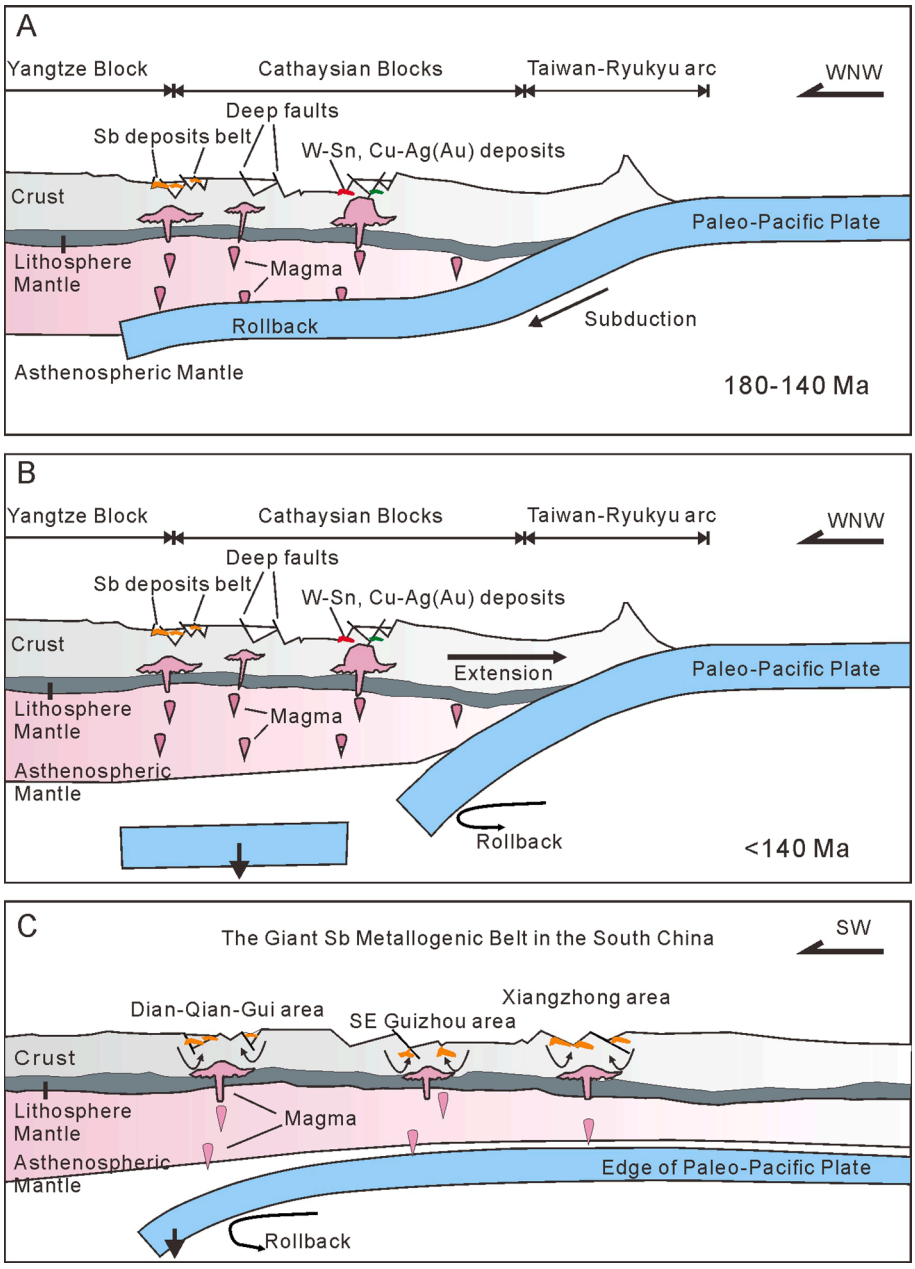

Fig. 12. A proposed dynamic model for the GSMB related to west-northwestward slab-flat subduction and followed rollback of Pacific plate in the Late Mesozoic. (A, B) The slab-flat subduction and post-subduction of paleo-Pacific Plate before and after 140 Ma not only generated the abundant igneous rocks and W-Sn, Cu-Au (Ag) deposits in Cathaysian Blocks, but also heated the basement and promoted the formation of the GSMB. (C) Deep intrusions started at the far end of the subduction slab and became younger towards the NE of the subduction zone and caused a chronology difference between Sb deposits in the Xiangzhong basin, the SE Guizhou area, and the Dian-Qian-Gui area.

identified (Fig. 11A; Zhou et al., 2006; Sun et al., 2007; Wang et al., 2011). Pacific plate subduction into the Eurasian continent during the Early Yanshanian (>140 Ma) and post-subduction during Late Yanshanian Period (140–70 Ma) is widely believed to be responsible for the formation of abundant granitic rocks in South China, with the most famous models including the low-angle subduction model (Zhou and Li, 2000; Zhou et al., 2006), flat-slab subduction model (Li and Li, 2007; Li et al., 2007) and large-scale extensional model (Mao et al., 2021a, Mao et al., 2021b). The low-angle subduction model interpreted that the overall southeastward migration of magmatism in Southeast China was a result of a northwest- to west-north- westward subduction of the Pacific oceanic lithosphere during the Late Mesozoic (Zhou and Li, 2000; Zhou et al., 2006). The flat-slab subduction model proposed that a flattened Pacific oceanic lithosphere that was caused by underflow of an oceanic plateau with a diameter of approximately 1000 km migrated further into the South China Block, followed by slab foundering (Li and Li, 2007; Li et al., 2007). The large-scale extensional model suggested that the subducted Paleo-Pacific plate was broken in the mantle transition zone in the deep of eastern China, and left a stagnant fragment in asthenospheric mantle during slab retreat. The eastern Asian continent margin undergone extension which led to the formation of related structure, metamorphism and magmatism (Mao et al., 2021a, Mao et al., 2021b). However, the drifting direction of the Paleo-Pacific plate changed several times, of which the major transition event occurred in 125–122 Ma when the drifting direction changed by 80° from southwest to northwest (Sun et al., 2007). Combining the younger trend northeastward of igneous rocks during 180–125 Ma (Fig. 11A; Zhou et al., 2006; Sun et al., 2007; Wang et al., 2011), Wang et al. (2011) proposed that a southwestward subduction was followed by a northeastward rollback of the Pacific oceanic slab.

In previous study Peng and Hu (2001) proposed a model of two-stage tectonic- magmatic activation to interpret the formation of the GSMB in the Southeast Yangtze Block, in which W-Sn-Zn-Pb and granite-related rare-metal deposits were considered to form at first stage (J_3-K_1) in South China, and the low-temperature deposits are formed at the second stage (K_2-E_1). However, the model is conflicted with the temporal

consistence between the Sb deposits in GSMB and the granite-related W-Sn polymetallic deposits in the Cathaysia block (Hu and Zhou, 2012; Mao et al., 2013; Hu et al., 2017a, Hu et al., 2017b). Furthermore, the ages of major large or giant Sb deposits in the GSMB, as investigated in this study, are mainly concentrated in a limited range (160–120 Ma) and show a consistent geochronological trend with those of igneous rocks in South China (Fig. 11B). Therefore, considering the presence of deep-seated granites in the GSMB revealed by geophysical data, we propose that the formation of the GSMB in southeastern edge of the Yangtze Block also was related to the subduction and post-subduction of the paleo-Pacific plate during Late Mesozoic, same as that of the igneous rocks and related W-Sn deposits in the Cathaysia block.

6. Dynamic model of Sb mineralisation in the GSMB

Based on the aforementioned discussion, we invoked a model of the west-northwestward slab-flat subduction and post-subduction of the paleo-Pacific plate during Late Mesozoic for the formation of the giant Sb metallogenic belt in South China. Firstly, the west-northwestward slab-flat subduction of the paleo-Pacific plate occurred during the transformation of the tectonic regimes in South China at ~ 180 Ma (Maruyama 1997; Zhou and Li, 2000; Scotese, 2002; Zhou et al., 2006; Wang et al., 2011). The subduction of the paleo-Pacific plate during 180–140 Ma and followed extensive crustal extension not only triggered large-scale magmatism and related W-Sn and Cu-Ag (Au) mineralisation in Cathaysia Block (Fig. 12A, B; Zhou et al., 2006; Li and Li, 2007; Wang et al., 2011; Sun et al., 2012; Mao et al., 2021a, b), but also produced extensive concealed magmatism in the GSMB, which display a younger trend from the Dian-Qian-Gui area towards the Xiangzhong area that is broadly consistent with the age distribution trend of the Sb deposits in the GSMB (Fig. 12C). Therefore, in combination of reported geological and geochemical data, a new geodynamic model for the formation of GSMB in South China can be invoked that assumes deep circulation of low-temperature and low-salinity crustal fluids through faults under an extensional tectonic setting during Late Mesozoic (160–120 Ma), mobilization of Sb and sulfur from the basement sequences and ascending along deep faults and subsequently deposition of Sb in or around fault/fracture zones (Fig. 12C). Concealed magmatism may have served as heat sources for circulation and transportation of crustal fluids to form Sb deposits in GSMB.

7. Summary and remaining issues

The GSMB in South China contains >500 Sb deposits with various scales and grades. Available studies suggest that the majority of large Sb deposits in the GSMB mainly formed during the Late Mesozoic (160–120 Ma), and the ages of these Sb deposits show a younger trend from southwest to northeast, which is similar to that of igneous rocks in the Cathaysia Block, implying that they formed under a similar geodynamic setting. The west-northwestward slab-flat subduction and post-subduction of the paleo-Pacific plate during the Late Mesozoic are probably responsible for both Sb deposits in the GSMB and igneous rocks and associated W-Sn deposits in South China. Deep-seated granitic magmatism that occurred during the subduction and rollback of the paleo-Pacific plate provided a heat source for the circulation of possible meteoric fluids and leaching of Sb from basement sequences to form Sb deposits in the GSMB. However, a critical issue is that the sources of huge Sb metal in these large Sb deposits remain poorly understood because the Sb content is relatively low (typically < 1–2 ppm) in the potential candidates of source rocks in this region (Ma et al., 2002; Hu, 2021), and further work is required to clarify the mechanisms of super-enrichment and transportation of Sb in hydrothermal systems to form large Sb deposits.

Declaration of Competing Interest

The authors declare that they have no known competing financial interests or personal relationships that could have appeared to influence the work reported in this paper.

Acknowledgements

This research was financially supported jointly by the projects of the National Natural Science Foundation of China (41903044, 41703044, 41830432 and U1812402) , the China Postdoctoral Science Foundation (2018M643531), and the Field Forefront Project of the State Key Laboratory of Ore Deposit Geochemistry, Institute of Geochemistry, Chinese Academy of Sciences (202102). We are very grateful to Prof. Jingwen Mao, Prof. Huan Li and another anonymous reviewer for their constructive comments and suggestions that helped to improve our manuscript.

References

Bai, D.Y., Jia, B.H., Wang, X.H., Peng, Y.Y., Jia, P.Y., Ling, Y.X., 2013. Kinematics of tectonic deformation of the western Xiangzhong Basin and its tectonic mechanism. Acta Geol. Sin. 87, 1791–1802 (in Chinese with English abstract).

Burnard, P.G., Polya, D.A., 2004. Importance of mantle derived fluids during granite associated hydrothermal circulation: He and Ar isotopes of ore minerals from Panasqueira. Geochim. Cosmochim. Acta. 68, 1607–1615.

Burnard, P.G., Hu, R., Turner, G., Bi, X.W., 1999. Mantle, crustal and atmospheric noble gases in Ailaoshan gold deposits, Yunnan Province, China. Geochim. Cosmochim. Acta. 63 (10), 1595–1604.

Cai, H.J., Zhang, B.G., Li, Y.S., 1997. Fluid inclusion geochemistry of antimony deposits in the border area between Yunnan, Guizhou and Guangxi. Acta Mineral. Sin. 17, 427–434 (in Chinese with English abstract).

Cai, J.-X., Zhang, K.-J., 2009. A new model for the Indochina and South China collision during the Late Permian to the Middle Triassic. Tectonophysics 467 (1-4), 35–43.

Charvet, J., Shu, L., Faure, M., Choulet, F., Wang, B.o., Lu, H., Breton, N.L., 2010. Structural development of the Lower Paleozoic belt of South China: genesis of an intracontinental orogen. J. Asian Earth Sci. 39 (4), 309–330.

Chen, X., Su, W.C., Huang, Y., 2016. He and Ar isotope geochemistry of ore-forming fluids for the Qinglong Sb deposit in Guizhou Province, China. Acta Petrol. Sin. 32, 3312–3320 (in Chinese with English abstract).

Chen, J., Yang, R.-D., Du, L.-J., Zheng, L.-L., Gao, J.-B., Lai, C.-K., Wei, H.-R., Yuan, M.-G., 2018. Mineralogy, geochemistry and fluid inclusions of the Qinglong Sb-(Au) deposit, Youjiang basin (Guizhou, SW China). Ore Geol. Rev. 92, 1–18.

Chu, Y., Faure, M., Lin, W., Wang, Q.C., Ji, W.B., 2012a. Tectonics of the Middle Triassic intracontinental Xuefengshan Belt, South China: new insights from structural and chronological constraints on the basal decollement zone. Int. J. Earth Sci. 101, 2125–2150.

Chu, Y., Lin, W., Faure, M., Wang, Q., Ji, W., 2012b. Phanerozoic tectonothermal events of the Xuefengshan Belt, central South China: implications from U-Pb age and Lu-Hf determinations of granites. Lithos 150, 243–255.

Cui, Y.L., 1995. Ore-forming material sources of the Dushan antimony deposit in Guizhou Province. Geol. Explor. Non-Ferrous Metals 4, 193–199 (in Chinese with English abstract).

Cui, Y.L., 1992. Geological character and mineralization conditions of Dushan Sb deposit, Guizhou. Master thesis, Kunming Engineering College (in Chinese with English abstract).

Davidheiser-Kroll, B., Stuart, F.M., Boyce, A.J., 2014. Mantle heat drives hydrothermal fluids responsible for carbonate-hosted base metal deposits: evidence from He-3/He-4 of ore fluids in the Irish Pb-Zn ore district. Miner. Depos. 49, 547–553.

Diao, L.P., Wang, Z.G., Wu, B.J., Xie, X.Y., 2017. Information analysis and optimization of ore targets in the Dushan antimony ore concentration area, Guizhou Province. Geol. China 44, 793–809 (in Chinese with English abstract).

Fan, D., Zhang, T., Ye, J., 2004. The Xikuangshan Sb deposit hosted by the Upper Devonian black shale series, Hunan, China. Ore Geol. Rev. 24 (1-2), 121–133.

Faure, M., Shu, L.S., Wang, B., Charvet, J., Choulet, F., Monié, P., 2009. Intracontinental subduction: a possible mechanism for the Early Paleozoic Orogen of SE China. Terr. Nova 21, 360–368.

Faure, M., Lepvrier, C., Nguyen, V.V., Vu, T.V., Lin, W., Chen, Z., 2014. The South China block-Indochina collision: where, when, and how? J. Asian Earth Sci. 79, 260–274.

Fu, S.L., Hu, R.Z., Chen, Y.W., Luo, J.C., 2016. Chronology of the Longshan Au Sb deposit in central Hunan Province: constraints from pyrite Re-Os and zircon U-Th/He isotopic dating. Acta Petrol. Sin. 32, 3507–3517 (in Chinese with English abstract).

Fu, S., Hu, R., Yan, J., Lan, Q., Gao, W., 2019. The mineralization age of the Banxi Sb deposit in Xiangzhong metallogenic province in southern China. Ore Geol. Rev. 112, 103033. https://doi.org/10.1016/j.oregeorev.2019.103033.

Fu, S., Hu, R., Yin, R., Yan, J., Mi, X., Song, Z., Sullivan, N.A., 2020a. Mercury and in situ sulfur isotopes as constraints on the metal and sulfur sources for the world's largest Sb deposit at Xikuangshan, southern China. Miner. Depos. 55 (7), 1353–1364.

Fu, S., Hu, R., Batt, G.E., Danišík, M., Evans, N.J., Mi, X., 2020b. Zircon (U-Th)/He thermochronometric constraints on the mineralization of the giant Xikuangshan Sb deposit in central Hunan, South China. Miner. Depos. 55 (5), 901–912.
Fu, S., Zajacz, Z., Tsay, A., Hu, R., 2020c. Can magma degassing at depth donate the metal budget of large hydrothermal Sb deposits? Geochim. Cosmochim. Acta 290, 1–15.
Fu, S.L., 2015. Genesis and chronology of Indosinian granites and genetic links to the Sb-Au mineralization in central Hunan Province (PhD thesis). The University of Chinese Academy of Sciences, Beijing, 1-116 (in Chinese with English abstract).
Galfetti, T., Bucher, H., Martini, R., Hochuli, P.A., Weissert, H., Crasquin-Soleau, S., Brayard, A., Goudemand, N., Brühwiler, T., Guodun, K., 2008. Evolution of Early Triassic outer platform paleoenvironments in the Nanpanjiang Basin (South China) and their significance for the biotic recovery. Sediment. Geol. 204 (1-2), 36–60.
Gu, X.X., Liu, J.M., Schulz, O., Vavtar, F., Zheng, M.H., 2004. Syngenetic origin of the Woxi W-Sb-Au deposit in Hunan: evidence from trace elements and sulfur isotopes. Chin. J. Geol. 39, 424–439.
Gu, X.X., Zhang, Y.M., Schulz, O., Vavtar, F., Liu, J.M., Zheng, M.H., Zheng, L., 2012. The Woxi W-Sb–Au deposit in Hunan, South China: an example of Late Proterozoic sedimentary exhalative (SEDEX) mineralization. J. Asian Earth Sci. 57, 54–75.
Han, Z., Wang, J., Li, C., Qiao, K., Chang, J., 2019. REE geochemistry of gangue minerals and their geological significance in the Muli antimony ore deposit in Yunnan, China. Acta Geochim. 38 (6), 848–862.
Hoefs, J., 2009. Stable Isotope Geochemistry. Springer, Berlin Heidelberg, pp. 573–576.
Hu, R.Z., 2021. Large Scale Low-temperature Metallogenesis in South China. Science Press, Beijing (in Chinese).
Hu, R.-Z., Burnard, P.G., Bi, X.-W., Zhou, M.-F., Peng, J.-T., Su, W.-C., Zhao, J.-H., 2009. Mantle-derived gaseous components in ore-forming fluids of the Xiangshan uranium deposit, Jiangxi Province, China: evidence from He, Ar and C isotopes. Chem. Geol. 266 (1-2), 86–95.
Hu, R.-Z., Chen, W.T., Xu, D.-R., Zhou, M.-F., 2017b. Reviews and new metallogenic models of mineral deposits in South China: an introduction. J. Asian Earth Sci. 137, 1–8.
Hu, R.Z., Peng, J.T., Ma, D.S., Su, W.C., Shi, C.H., Bi, X.W., Tu, G.C., 2007. Epoch of large-scale low-temperature mineralizations in southwestern Yangtze massif. Mineral Depos. 26, 583–596 (in Chinese with English abstract).
Hu, R.Z., Fu, S.L., Xiao, J.F., 2016. Major scientific problems on low-temperature metallogenesis in South China. Acta Petrol. Sin. 32, 3239–3251 (in Chinese with English abstract).
Hu, R., Fu, S., Huang, Y., Zhou, M.-F., Fu, S., Zhao, C., Wang, Y., Bi, X., Xiao, J., 2017a. The giant South China Mesozoic low-temperature metallogenic domain: reviews and a new geodynamic model. J. Asian Earth Sci. 137, 9–34.
Hu, X.W., Pei, R.F., Zhou, S., 1996. Sm-Nd dating for antimony mineralization in the Xikuangshan deposit, Hunan, China. Res. Geol. 46, 227–231.
Hu, A.X., Peng, J.T., 2018. Fluid inclusions and ore precipitation mechanism in the giant Xikuangshan mesothermal antimony deposit, South China: conventional and infrared microthermometric constraints. Ore Geol. Rev. 95, 49–64.
Hu, R.-Z., Zhou, M.-F., 2012. Multiple Mesozoic mineralization events in South China—an introduction to the thematic issue. Miner. Depos. 47 (6), 579–588.
John, B.M., Zhou, X.H., Li, J.L., 1990. Formation and tectonic evolution of Southeastern China and Taiwan: isotopic and geochemical constraints. Tectonophysics 183 (1-4), 145–160.
Li, S.S., 1996. Evolution of antimony mineralization by the mantle plume of deep fluid in central Hunan. Hunan Geol. 15, 137–142 (in Chinese with English abstract).
Li, H.T., Cao, D.Y., Wang, L.J., Guo, A.J., Li, Y.F., Xu, H., 2013. Characteristics and evolution of coal-controlled structures on the east slope of the Xuefengshan domain in central Hunan Province. Geotect. Metall. 37, 611–621 (in Chinese with English abstract).
Li, H., Kong, H., Zhou, Z.-K., Tindell, T., Tang, Y.-Q., Wu, Q.-H., Xi, X.-S., 2019. Genesis of the Banxi Sb deposit, South China: constraints from wall-rock geochemistry, fluid inclusion microthermometry, Rb-Sr geochronology, and H-O-S isotopes. Ore Geol. Rev. 115, 103162. https://doi.org/10.1016/j.oregeorev.2019.103162.
Li, H., Danišík, M., Zhou, Z.-K., Jiang, W.-C., Wu, J.-H., 2020. Integrated U-Pb, Lu-Hf and (U-Th)/He analysis of zircon from the Banxi Sb deposit and its implications for the low-temperature mineralization in South China. Geosci. Front. 11 (4), 1323–1335.
Li, X.-H., Li, Z.-X., Li, W.-X., Liu, Y., Yuan, C., Wei, G., Qi, C., 2007. U-Pb zircon, geochemical and Sr-Nd-Hf isotopic constraints on age and origin of Jurassic I- and A-type granites from central Guangdong, SE China: a major igneous event in response to foundering of a subducted flat-slab? Lithos 96 (1-2), 186–204.
Li, Z.-X., Li, X.-H., 2007. Formation of the 1300-km-wide intracontinental orogen and postorogenic magmatic province in Mesozoic South China: a flat-slab subduction model. Geology 35 (2), 179–182.
Li, Z.-X., Li, X.-H., Chung, S.-L., Lo, C.-H., Xu, X., Li, W.-X., 2012a. Magmatic switch-on and switch-off along the South China continental margin since the Permian: transition from an Andean-type to a Western Pacific-type plate boundary. Tectonophysics 532-535, 271–290.
Li, H.e., Ling, M.-X., Li, C.-Y., Zhang, H., Ding, X., Yang, X.-Y., Fan, W.-M., Li, Y.-L., Sun, W.-D., 2012b. A-type granite belts of two chemical subgroups in central eastern China: indication of ridge subduction. Lithos 150, 26–36.
Li, H., Wu, Q.-H., Evans, N.J., Zhou, Z.-K., Kong, H., Xi, X.-S., Lin, Z.-W., 2018. Geochemistry and geochronology of the Banxi Sb deposit: implications for fluid origin and the evolution of Sb mineralization in central-western Hunan, South China. Gondwana Res. 55, 112–134.
Li, J.H., Zhang, Y.Q., Dong, S.W., Ma, Z.L., Li, Y., 2015. LA-MC-ICPMS zircon U-Pb geochronology of the Hongxiaqiao and Banshanpu granitoids in Eastern Hunan Province and its geological implications. Acta Geosci. Sin. 36, 187–196 (in Chinese with English abstract).
Liang, B.R., Zhang, Z.R., 1986. A study on the typomorphic properties of Quartz in Woxi Au-Sb-W deposit, Western Hunan. Hunan Geol. 5, 17–25 (in Chinese).
Lin, F.M., 2014. On the Ore-forming Fluid in the Xikuangshan Antimony Deposit, Central Hunan. Master's thesis, Central South University, China, 1-70 (in Chinese with English abstract).
Liu, Z.H., 2005. Sedimentary facies differentiation and its mechanism during Permian in central-southern Hunan. Chinese J. Geol. 40, 510–517 (in Chinese with English abstract).
Liu, J.M., Gu, X.X., Liu, J.J., Zheng, M.H., 1998. Giant metallogenic Sb belt in South China and its constraints. Acta Geophys. Sin. 41, 206–215 (in Chinese with English abstract).
Liu, G.M., Jian, H.M., 1983. Geological characteristics of the Xikuangshan antimony ore field. Mineral Depos. 2, 43–49 (in Chinese with English abstract).
Liu, S., Su, W., Hu, R., Feng, C., Gao, S., Coulson, I.M., Wang, T., Feng, G., Tao, Y., Xia, Y., 2010. Geochronological and geochemical constraints on the petrogenesis of alkaline ultramafic dikes from southwest Guizhou Province, SW China. Lithos 114, 253–264.
Lu, Y.L., Peng, J.T., Yang, J.H., Hu, A.X., Li, Y.K., Tan, H.Y., Xiao, Q.Y., 2017. Petrogenesis of the Ziyunshan pluton in central Hunan, South China: constranits from zircon U-Pb dating, element geochemistry and Hf-O isotopes. Acta Petrol. Sin. 33, 1705–1728 (in Chinese with English abstract).
Luo, X.L., Yi, S.J., Liang, J.C., 1984. Ore genesis of the Woxi Au–Sb deposit, western Hunan. Geol. Prospect. 20, 1–10 (in Chinese).
Ma, D.S., 2008. Metallogenetic characteristics of the important deposits in South China. Bullet. Miner. Petrol. Geochem. 27, 209–217 (in Chinese with English abstract).
Ma, D.S., Pan, J.Y., Xie, Q.L., He, J., 2002. Ore source of Sb (Au) deposits in Center Hunan: I.Evidences of trace elements and experimental geochemistry. Mineral Depos. 3, 366–376 (in Chinese with English abstract).
Ma, D.S., Pan, J.Y., Xie, Q.L., 2003. Ore Sources of Sb(Au) Deposits in Central Hunan:II. Evidence of Isotopic Geochemistry. Mineral Depos. 22, 78–87 (in Chinese with English abstract).
Mao, J.W., Cheng, Y.B., Chen, M.H., Pirajno, F., 2013. Major types and time-space distribution of Mesozoic ore deposits in South China and their geodynamic settings. Miner. Depos. 48 (3), 267–294.
Mao, J., Liu, P., Goldfarb, R.J., Goryachev, N.A., Pirajno, F., Zheng, W., Zhou, M., Zhao, C., Xie, G., Yuan, S., Liu, M., 2021b. Cretaceous large-scale metal accumulation triggered by post-subductional large-scale extension, East Asia. Ore Geol. Rev. 136, 104270.
Mao, J.W., Zheng, W., Xie, G.Q., Lehmann, L., Goldfarb, R., 2021a. Recognition of a Middle-Late Jurassic arc-related porphyry copper belt along the southeast China coast: geological characteristics and metallogenic implications. Geology 49, 592–596.
Mark, D.F., Stuart, F.M., de Podesta, M., 2011. New high-precision measurements of the isotopic composition of atmospheric argon. Geochim. Cosmochim. Acta 75 (23), 7494–7501.
Maruyama, S., 1997. Pacific-type orogeny revisited: Miyashiro-type orogeny proposed. Island Arc 6 (1), 91–120.
Ohmoto, H., Rye, R.O., 1979. Isotopes of sulfur and carbon. In: Barnes, H.L. (Ed.), Geochemistry of Hydrothermal Ore Deposits, 2nd edn. John Wiley and Sons, New York, pp. 509–567.
Pan, J.Q., Wu, D.H., 2017. Comparison of sources for the ore-forming fluids and materials for the antimony ore deposits in south and southwest of Guizhou Province, China. Geol. Sic. Techn. Inform. 36, 123–132 (in Chinese with English abstract).
Peng, Y., Gu, X., Zhang, Y., Liu, L.i., Wu, C., Chen, S., 2014. Ore-forming process of the Huijiabao gold district, southwestern Guizhou Province, China: evidence from fluid inclusions and stable isotopes. J Asian Earth Sci. 93, 89–101.
Peng, J.T., Hu, R.Z., 2001. Metallogenic epoch and metallogenic tectonic environment of antimony deposits, south china. Geol.-Geochem. 29, 104–108 (in Chinese with English abstract).
Peng, J.T., Hu, R.Z., Burnard, P.G., 2003a. Samarium-neodymium isotope systematics of hydrothermal calcite from the Xikuangshan antimony deposit (Hunan, China): the potential of calcite as a geochronometer. Chem. Geol. 200, 129–136.
Peng, J.T., Hu, R.Z., Jiang, G.H., 2003b. Strontium Isotope Geochemistry of Fluorites from Qinglong Antimony Deposit in Guizhou Province. Geol. J. China Universities 9, 244–251 (in Chinese with English adstract).
Peng, J.T., Hu, R.Z., Zou, L.Q., Liu, J.X., 2002. Isotope tracing of ore-forming materials for the Xikuangshan antimony deposit, central Hunan. Acta Miner. Sin. 22, 155–159 (in Chinese with English abstract).
Peng, B.X., Wang, Y.J., Fan, W.M., Peng, T.P., 2006. LA-ICPMS zircon U-Pb dating and significances of three typical granitic rocks in Central Hunan and western Guangxi. Acta Geol. Sin. 10, 1597 (in Chinese).
Peng, J.T., Zhang, D.L., Hu, R.Z., Wu, M.J., Lin, Y.X., 2008. Sm-Nd and Sr Isotope Geochemistry of Hydrothermal Scheelite from the Zhazixi W-Sb Deposit, Western Hunan. Acta Geol. Sin. 82, 1514–1521 (in Chinese with English abstract).
Pi, Q., Hu, R., Xiong, B., Li, Q., Zhong, R., 2017. In situ SIMS U-Pb dating of hydrothermal rutile: reliable age for the Zhesang Carlintype gold deposit in the golden triangle region, SW China. Mine. Depos. 52 (8), 1179–1190.
Rao, J.R., Luo, J.L., Yi, Z.J., 1999. The mantle-crustal tectonic metallogenic model and ore-prospecting prognosis in the Xikuangshan antimony ore field. Geophys. Geoche. Explor. 23, 241–249 (in Chinese with English abstract).
Scotese, C.R., 2002. http://www.scotese.com, (PALEOMAP website).
Shen, N.P., Peng, J.T., Yuan, S.D., Zhang, D.L., Hu, R.Z., Wang, G.Q., 2008. Characteristics of fluid inclusions in Xujiashan antimony deposit of Hubei Province and its implications. Mineral Depos. 27, 570–578 (in Chinese with English abstract).
Shen, N.P., Su, W.C., Fu, Y.Z., Xu, C.X., Yang, J.H., Cai, J.L., 2013. Characteristics of Sulfur and Lead Isotopes for Banian Antimony Deposit in Dushan Area, Guizhou

Province, China: implication for Origin of Ore-forming Materials. Acta Mineral. Sin. 33, 271–277 (in Chinese with English abstract).
Shi, M.K., Fu, B.Q., Jin, X.X., 1993. Antimony Metallogeny in Central Part of Hunan Province. Hunan Press of Science and Technology, Changsha, pp. 1–151 (in Chinese).
Shu, L.S., 2006. Pre-Devonian tectonic evolution of south China from Cathaysian Block to Caledonian Period folded orogenic belt. Geol. J. China Uni. 12, 418–431 (in Chinese with English abstract).
Shu, L.S., 2012. An analysis of principal features of tectonic evolution in South China Block. Geol. Bull. China 31, 1035–1053 (in Chinese with English abstract).
Shu, L.S., Zhou, X.M., Deng, P., Wang, B., Jiang, S.Y., Yu, J.H., Zhao, X.X., 2009. Mesozoic tectonic evolution of the southeast China Block: new insights from basin analysis. J. Asian Earth Sci. 34 (3), 376–391.
Song, C.A., Feng, Z.H., Lei, L.Q., 2009. Geotectonic metallogenic evolution and belt of Tin polymetal ore and exploration in Guangxi. J. Guilin Univers. Technol. 29, 207–215 (in Chinese with English abstract).
Stuart, F.M., Turner, G., Duckworth, R.C., Fallick, A.E., 1994. Helium isotopes as tracers of trapped hydrothermal fluids in ocean-floor sulfides. Geology 22 (9), 823–826.
Su, W.C., Zhu, L.Y., Ge, X., Shen, N.P., Zhang, X.C., Hu, R.Z., 2015. Infrared microthermometry of fluid inclusions in stibnite from the Dachang antimony deposit, Guizhou. Acta Petrol. Sin. 31, 918–924 (in Chinese with English abstract).
Sun, W., Ding, X., Hu, Y.-H., Li, X.-H., 2007. The golden transformation of the Cretaceous plate subduction in the west Pacific. Earth Planet. Sci. Lett. 262 (3-4), 533–542.
Sun, W.-D., Yang, X.-Y., Fan, W.-M., Wu, F.-Y., 2012. Mesozoic large scale magmatism and mineralization in South China: preface. Lithos 150, 1–5.
Sun, J., Zhou, C., Lu, W., Guo, A.M., Xiao, R., Wei, H.T., Tan, S.M., Jia, P.Y., 2020. He-Ar-Sr Isotope Geochemistry of Ore-forming Fluids in the Gutaishan Au-Sb Deposit in Hunan Province and Its Significance for Deep Prospecting. Acta Geoscient. Sin. 41, 267–279 (in Chinese with English abstract).
Wang, L.J., 1994. The genesis of Muli antimony deposit, Yunnan. J. Guilin College Geol. 14, 350–354 (in Chinese with English abstract).
Wang, X.Q., 1995. Geochemical characteristics of the Dushan reworked antimony deposit, Guizhou. Geol. Rev. 41, 61–73 (in Chinese with English abstract).
Wang, D.H., Chen, Z.H., Chen, Y.C., Tang, J.X., Li, J.K., Ying, L.J., Wang, C.H., Liu, S.B., Li, L.X., Qin, Y., Li, H.Q., Qu, W.J., Wang, Y.B., Chen, W., Zhang, Y., 2010. New Data of the Rock-Forming and Ore-Forming Chronology for China's Important Mineral Resources Areas. Acta Geol. Sin. 84, 1030–1040 (in Chinese with English abstract).
Wang, Y.L., Chen, Y.C., Wang, D.H., Xu, J., Chen, Z.H., Liang, T., 2013. The principal antimony concentration areas in China and their resource potentials. Geol. China 40, 1366–1378 (in Chinese with English abstract).
Wang, X.Q., Cui, Y.L., 1996. Geology and mineralization characteristics of Banian Sb deposit, Guizhou. Miner. Geol. Southwest China 10, 22–31 (in Chinese).
Wang, Z.Q., Gao, Z.L., Ding, X.Z., Huang, Z.Z., 2012. Tectonic environment of the metamorphosed basement in the Jiangnan Orogen and its evolutional features. Geol. Rev. 58, 401–413 (in Chinese with English abstract).
Wang, X.Q., Jin, S.C., 1994. Geology of Dushan Sb deposit, Guizhou. Yunnan Science and Technology Press, Kunming (in Chinese).
Wang, Y.J., Li, Z.X., 2003. History of Neoproterozoic rift basins in South China: implications for Rodinia break-up. Precambrian Res. 122, 141–158.
Wang, F.-Y., Ling, M.-X., Ding, X., Hu, Y.-H., Zhou, J.-B., Yang, X.-Y., Liang, H.-Y., Fan, W.-M., Sun, W., 2011. Mesozoic large magmatic events and mineralization in SE China: oblique subduction of the Pacific plate. Int. Geol. Rev. 53 (5-6), 704–726.
Wang, J.Q., Shu, L.S., Santosh, M., 2016. Petrogenesis and tectonic evolution of Lianyunshan complex, South China: insights on Neoproterozoic and late Mesozoic tectonic evolution of the central Jiangnan Orogen. Gondwana Res. 39, 114–130.
Wang, Y., Wang, D.H., Wang, Y.L., Huang, F., 2020. Quantitative Research on Metallogenic Regularities of Antimony Deposits in China Based on Geological Big Data. Geol. China 48, 52–67 (in Chinese with English abstract).
Wang, L., Zhang, Y.W., Liu, S.G., 2009. The application of regional gravity and magnetic data to delineating intrusive bodies and local geological structures in Guizhou Province. Geophys. Geochem. Explor. 33, 246–249 (in Chinese with English abstract).
Wang, L., Long, C.L., Liu, Y., 2015. Discussion on concealed rock mass delineation and gold source in southwestern Guizhou. Geoscience 29, 703–712 (in Chinese with English abstract).
Wang, Q., Zhao, Z.H., Jian, P., Xu, J.F., Bao, Z.W., Ma, J.L., 2004. SHRIMP zircon geochronology and Nd-Sr isotopic geochemistry of the Dexing granodiorite porphyries. Acta Petrol. Sin. 20, 315–324 (in Chinese with English abstract).
Wang, D.M., 2012. A Study on the characteristic and Origin of the Antimony Deposit in Danchi Metallogenic Belt Guangxi. Master Dissertation, Chang'an University (in Chinese with English abstract).
Wei, W.Z., 1993. Geological characteristics of Maxiong Sb deposit. Miner. Geol. Southwest China 2, 8–16 (in Chinese).
Wong, J., Sun, M., Xing, G.F., Li, X.H., Zhao, G.C., Wong, K., Yuan, C., Xia, X.P., Li, L.M., Wu, F.Y., 2009. Geochemical and zircon U-Pb and Hf isotopic study of the Baijuhuajian metaluminous A-type granite: extension at 125–100 Ma and its tectonic significance for South China. Lithos 112, 289–305.
Xiao, Q.M., Zeng, D.R., Jin, F.Q., Yang, M.Y., Yang, Z.F., 1992. Time-Space distribution feature and exploration guide of China's Sb-Deposits. Geol. Explor. 12, 9-14(in Chinese with English abstract).
Xiao, X.G., 2014. Geochronology, ore geochemistry and genesis of the Banpo antimony deposit, Guizhou Province, China PhD thesis. Kunming University of Science and Technology, Kunming, 1-138 (in Chinese with English abstract).
Xie, Q.L., Ma, D.S., Liu, Y.J., 1996. Geochemical characteristics of calcite in the Xikuangshan antimony deposit, Hunan. Miner. Res. Geol. 10, 94–99 (in Chinese with English abstract).
Xu, L., Lehmann, B., Mao, J., Nägler, T.F., Neubert, N., Böttcher, M.E., Escher, P., 2012. Mo isotope and trace element patterns of Lower Cambrian black shales in South China: multi-proxy constraints on the paleoenvironment. Chem. Geol. 318-319, 45–59.
Xu, Z.Y., Yao, G.S., Guo, Q.X., Chen, Z.L., Dong, Y., Wang, P.W., Ma, L.Q., 2010. Genetic interpretation about geotectonics and structural transfiguration of the southern Guizhou depression. Geotecton. Metall. 34, 20–31 (in Chinese with English abstract).
Xue, H.F., Chen, X.L., Yang, Z.K., Zheng, M.H., 2019. The trike-slip tectonic system ore-controlling characteristics of the Banpo-Banian fault in Dushan antimony orefield. Guizhou. Miner. Res. Geol. 33, 1–9 (in Chinese with English abstract).
Yang, S.Q., 1986. On inquiry about the genesis of Hunan stibnite ore and the direction of ore search. Hunan Geol. 5, 12–25 (in Chinese).
Yang, J., Cawood, P.A., Du, Y., Huang, H.u., Hu, L., 2012. Detrital record of Indosinian mountain building in SW China: provenance of the Middle Triassic turbidites in the Youjiang Basin. Tectonophysics 574-575, 105–117.
Yang, D.S., Shimizu, M., Shimazaki, H., Li, X.H., Xie, Q.L., 2006. Sulfur isotope geochemistry of the supergiant Xikuangshan Sb deposit, central Hunan, China: constraints on sources of ore constituents. Res. Geol. 56, 385-396.
Yang, Z.Z., Lu, X.W., Qiu, H., 1998. Stable isotope geochemistry of Xikuangshan Sb deposit. J. Xi'an Engin. Univ. 20, 1–5 (in Chinese).
Yin, J.P., Dai, T.G., 1999. Source of ore-forming materials, metallogenic mechanism and prospecting significance of the Xikuangshan super large antimony deposit. Geol. Explor. Non-Ferrous Metals 8, 476–481 (in Chinese with English abstract).
Zaw, K., Peters, S.G., Cromie, P., Burrett, C., Hou, Z., 2007. Nature, diversity of deposit types and metallogenic relations of South China. Ore Geol. Rev. 31 (1-4), 3–47.
Zhang, GuoWei, Guo, AnLin, Wang, YueJun, Li, SanZhong, Dong, YunPeng, Liu, ShaoFeng, He, DengFa, Cheng, ShunYou, Lu, RuKui, Yao, AnPing, 2013. Tectonics of South China Continent and its implications. Sci. China: Earth Sci. 56 (11), 1804–1828.
Zhang, T.Y., Li, C.Y., Sun, S.J., Hao, X.L., 2020. Geochemical characteristics of antimony and genesis of antimony deposits in South China. Acta Petrol. Sin. 36, 44–54 (in Chinese with English abstract).
Zhang, X.J., Xiao, J.F., 2014. Zircon U-Pb geochronology, Hf isotope and geochemistry study of the Late Permian diabases in the northwest Guangxi autonomous region. Bull. China Society Miner. Petrol. Geochem. 33, 163–176 (in Chinese with English abstract).
Zhang, L., Yang, L.-Q., Groves, D.I., Sun, S.-C., Liu, Y.u., Wang, J.-Y., Li, R.-H., Wu, S.-G., Gao, L., Guo, J.-L., Chen, X.-G., Chen, J.-H., 2019. An overview of timing and structural geometry of gold, gold-antimony and antimony mineralization in the Jiangnan Orogen, southern China. Ore Geol. Rev. 115, 103173.
Zhang, G.L., Yao, J.Y., Gu, X.P., 1998. Time and spatial distribution regularities and deposit types of antimony in china. Miner. Res. Geol. 12, 306–312 (in Chinese with English abstract).
Zhao, J.H., Zhou, M.F., Yan, D.P., Zheng, J.P., Li, J.W., 2011. Reappraisal of the ages of Neoproterozoic strata in South China: no connection with the Grenvillian orogeny. Geology 39, 299-302.
Zhao, J.H., Peng, J.T., Hu, R.Z., Fu, Y.Z., 2005. Chronology, Petrology, Geochemistry and Tectonic Environment of Banxi Quartz Porphyry Dikes, Hunan Province. Acta Geosci. Sin. 26, 525–534 (in Chinese with English abstract).
Zheng, M.H., Chen, X.L., Yang, Z.K., Xue, H.F., 2019. Analysis on tectonic ore-controlling action in Dushan antimony orefield, Guizhou Province. Miner. Res. Geol. 33, 63–69 (in Chinese with English abstract).
Zhong, Y.F., Ma, C.Q., Yu, Z.B., Lin, G.C., Xu, H.J., Wang, R.J., Yang, K.G., Liu, Q., 2005. SHRIMP U-Pb zircon geochronology of the Jiuling granitic complex batholith in Jiangxi Province. Earth Sci. J. China Univ. Geosci. 30, 685–691 (in Chinese with English abstract).
Zhou, X.M., Li, W.X., 2000. Origin of Late Mesozoic igneous rocks in Southeastern China: implications for lithosphere subduction and underplating of mafic magmas. Tectonophysics 326 (3-4), 269–287.
Zhou, X., Sun, T., Shen, W., Shu, L., Niu, Y., 2006. Petrogenesis of Mesozoic granitoids and volcanic rocks in South China: A response to tectonic evolution. Episode 29 (1), 26–33.
Zhu, J.-J., Hu, R.-Z., Richards, J.P., Bi, X.-W., Stern, R., Lu, G., 2017. No genetic link between Late Cretaceous felsic dikes and Carlin-type Au deposits in the Youjiang basin, Southwest China. Ore Geol. Rev. 84, 328–337.
Zhu, Y.-N., Peng, J.-T., 2015. Infrared microthermometric and noble gas isotope study of fluid inclusions in ore minerals at theWoxi orogenic Au–Sb–Wdeposit, western Hunan, South China. Ore Geol. Rev. 65, 55–69.
Zhu, J.J., Zhong, H., Xie, G.Q., Zhao, C.H., Xu, L.L., Lu, G., 2016. Origin and geological implication of the inherited zircon from felsic dikes, Youjiang Basin, China. Acta Petrol. Sin. 32, 3269–3280 (in Chinese with English abstract).